Fondata nel 1241

University of Siena

Ph.D in Medical Genetics

FOXG1 and Rett Syndrome: functional characterization and set-up of an *in vitro* human cellular model

Roberta De Filippis

Supervisor: Prof. Alessandra Renieri

Academic year 2010-2011

Alla saggezza dei miei nonni

INDEX

ABSTRACT

FOXG1 gene encodes for a fork-head box protein G1, a transcription factor acting primarily as transcriptional repressor through DNA binding. In 2007, by array-CGH analysis in patients with Rett-like phenotype, we identified *FOXG1* as the third gene responsible for Rett Syndrome (RTT).

To clarify the clinical phenotype associated to *FOXG1* mutation, I performed molecular analysis of the gene including an international cohort of patients and 4 new cases were identified.

At the cellular level, FoxG1 is localized in the nucleus and it is dynamically involved in global chromatin regulation. Functional characterization of the protein revealed that FoxG1-binding to chromatin is reversible even if a significant fraction of the total protein is stably bound. Interestingly, analysis of mutated derivatives revealed specific alterations in FoxG1/chromatin interaction

During early neurodevelopment, FoxG1 is essential for the correct neurogenesis of the telencephalic progenitors cells. However, the protein is still expressed in post natal tissue suggesting that its function could be essential also in post-mitotic neurons. To unravel FoxG1 function in post-natal brain we thus decided to perform expression profiling experiments in $Foxg1^{+/-}$ heterozygous mice and some interesting genes were identified.

Up to now, studies on animal models have contributed to understand neural development, but, considering the high complexity of the human brain, these models appear limitative so that the need of an human neural model comes out. Recently, promising results for the study of neurodevelopmental disorders have been obtained by the application of iPS technology.

To investigate FoxG1 function at neuronal level, we thus set up the reprogramming protocol in our laboratory in order to obtain iPS cells starting from fibroblasts isolated from *FOXG1*-mutated patients with the final aim to differentiate them into neurons. This approach gives the opportunity to obtain *in vitro* affected neurons from a specific individual bypassing all legal and ethic limitations. Moreover, this approach open the way to patient-specific drug screening since obtained cells are genetically identical to the patient from whom they have been generated.

1. INTRODUCTION

Rett Syndrome (RTT, OMIM# 312750) is a progressive neurodevelopmental disorder that represents one of the most common causes of mental retardation in females. It was first described by Andreas Rett in 1966 [1], but the syndrome was internationally recognized in 1983 after the publication by Hagberg et al. in Annals of Neurology [2]. RTT is unique among genetic, chromosomal and other developmental disorders because of its usually sporadic occurrence, extreme female gender bias (incidence of 1:10000 female births), and peculiar clinical course with early normal development and subsequent regression, autonomic dysfunction, stagnation in brain growth and distinctive neuropathology [3]. According to the criteria of Hagberg, classical and atypical RTT cases can be distinguished. The clinical presentation of the atypical forms of RTT ranges from milder phenotypes with a later onset to more severe manifestations. These variants include:

i)   the early-onset seizures variant;

ii)   the "forme fruste";

iii)   the congenital variant;

iv)   the late regression variant;

v)   the Zappella variant (previously known as the Preserved Speech Variant; PSV).

About 99% of RTT cases are sporadic and they are mainly caused by mutations in the *MECP2* (Methyl-CpG-binding-protein 2) gene located on Xq28. Mutations in *MECP2* are reported in about 95% of cases with classic RTT and in a lower percentage (20-40%) of variant patients [4].

Mutations in *MECP2* gene have been described also in male patients with variable phenotype. In 2000, our group reported a family in which a *MECP2* mutation segregated in male patients with recessive X-linked mental retardation (XLMR) and spasticity [5]. Other studies reported *MECP2* mutations in patients with non specific mental retardation, severe neonatal encephalopathy, language disorder and schizophrenia, with psychosis, pyramidal signs and macro-orchidism (PPM-X), with Angelmann syndrome (AS) and with infantile autism [6, 7-9]. The wide spectrum of mutation types described in several databases (i.e. http://mecp2.chw.edu.au/; http://www.biobank.unisi.it) [10] includes missense, nonsense and

frameshift mutations with over 300 unique pathogenic nucleotide changes as well as deletions encompassing whole exons [11,12].

MECP2 gene (OMIM #300005) encodes for methyl-CpG-binding protein 2, which operates as a transcriptional regulator (both as activator and repressor) binding to methylated CpG dinucleotide islands of target genes via its methyl-CpG binding domain (MBD) and recruiting chromatin remodeling proteins via its transcription repressor domain (TRD) (Fig.1) [13]. In particular, MeCP2-mediated gene silencing occurs through chromatin modifications mediated by its interaction with Sin3A/HDACI or Ski/NcoR/HDACII repression complexes that remodel chromatin, which becomes inaccessible to the transcriptional machinery [14,15].

Figure 1. MeCP2 protein structure with its functional domains: methyl binding domain (MBD), transcription repression domain (TRD), nuclear localisation signal (NLS), C-terminal domain (C-ter). The numbers refer to the aminoacid positions.

In addition, MeCP2 is able to inhibit transcription directly at the level of the pre-initiation complex through the interaction of the TRD with the transcription factor TFIIB [16]. MeCP2 is also implicated in maintaining imprinting through chromatin looping [17]. Moreover, it has been demonstrated that it also interacts *in vivo* with the RNA-binding protein Y box-binding protein 1 (YB1) to regulate splicing of reporter constructs [18]. Finally, a recent study performed by sequential ChIP (seqChIP) analysis, demonstrated that MeCP2 acts as gene activator taking part to a multiprotein complex with the transcriptional activator CREB1 [19].

The identification of cases clinically compatible with RTT or its variants but negative for *MECP2* mutations, suggested the existence of additional RTT loci supporting the idea of genetic heterogeneity. Accordingly, in 2005, alterations in *CDKL5* (Cyclin-dependent Kinase like 5 also known as serine threonine kinase 9-STK9; OMIM #300203) gene were found in patients with the early onset seizures variant of RTT [20-25]. Mutations in this gene have been subsequently associated also to other severe neurodevelopmental disorders including infantile spasms, encephalopathy and West-syndrome.

CDKL5 gene encodes for a protein belonging to the serine-threonine kinase family, which shares homology with members of the mitogen-activated protein and cyclin dependent kinase (CDK) families [26]. Cdkl5 protein is able to shuttle between nucleus and cytoplasm and its subcellular distribution seems to be modulated by its C-terminal tail, which is responsible for an active nuclear export mechanism [27]. Moreover this terminal tail seems to act as a

negative regulator of the catalytic activity of Cdkl5 and probably this function is enclosed in the last 240 aminoacids [28,29] (Fig.2).
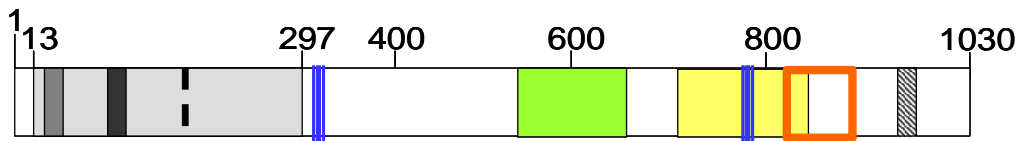
Figure 2. Schematic representation of the Cdkl5 protein. The catalytic kinase domain (grey box) contains an ATP binding site (dark grey box) and the serine–threonine protein kinase active site (black box). The Thr-Glu-Tyr (TEY) motif in this domain is indicated by a black dashed line. The Putative NLS are indicated with blue lines. The MeCP2 interaction domain (green box), and the DNMT1 interaction domain (yellow box) are also indicated. The orange square corresponds to the nuclear export signal. The signal peptidases I Serine active site, located in the C-terminal region of the protein, is represented by the striped box. Numbers at the top refer to aminoacid positions.

The observation that mutations in *MECP2* and *CDKL5* cause similar phenotypes suggested that the corresponding proteins may be involved in the same molecular pathway. In keeping with this hypothesis, previous studies comparing the expression patterns of Mecp2 and Cdkl5 in embryonic and postnatal mouse brains demonstrated that the two genes have an overlapping temporal and spatial expression profile during neuronal maturation and synaptogenesis. Moreover, the two proteins physically interact and Cdkl5 is indeed a kinase able to phosphorylate itself and to mediate MeCP2 phosphorilation, at least *in vitro* [22] (Fig. 3). In addition, very recent data evidenced that *in vivo* Mecp2 directly interacts with Cdkl5 gene in a methylation-dependent manner and that the over-expression of Mecp2 in transfected cells results in the repression of Cdkl5. These results reinforced the view of a possible overlapping phenotype in case of mutations in the two genes [30]
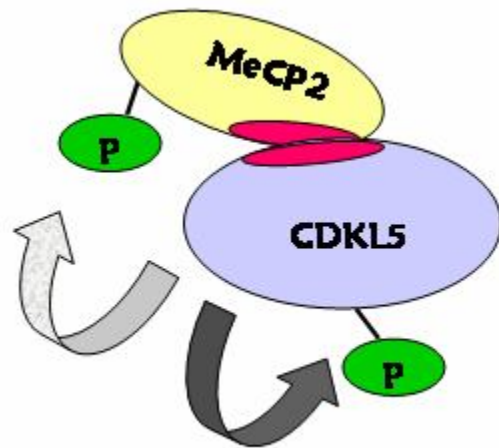
Figure 3: Interaction between Cdkl5 and MeCP2. A region of MeCP2 including the last residues of the TRD and residues belonging to the C-terminal domain represents the main interacting surface (red circle). Cdkl5 is a kinase able to phosphorylate itself and to mediates the phosphorylation of MeCP2 *in vitro*. The green circles represent phosphate groups.

In spite of the identification of *CDKL5* as a new RTT gene, a percentage of patients, especially among RTT variants, still missed a molecular defect. The molecular cause of another RTT variant, the congenital one, was identified in July 2008, when point mutations in *FOXG1* (Forkhead box protein G1; OMIM#164874) gene were identified in two girls affected by this severe variant. The affected girls presented the same clinical features of classic RTT but they appeared floppy and retarded since the very firs months of life [31].

1.1 Clinical Features

Currently, the diagnosis of RTT is based on defined clinical criteria which have been slightly modified over time to reflect increased understanding of disease features [32]. For classic RTT, these criteria include a period of apparently normal development, during which patients acquire motor, language and social milestones at the expected rate and age. Their neurological development is then arrested and patients undergo a period of regression, characterized by four stages (Fig. 4). During Stage I (6-18 months), patients stop to acquire new skills. Head growth decelerates, usually leading to acquired microcephaly, and patients show autistic features. During Stage II (1-4 years), girls lose the ability to speak and the purposeful use of hands. This stage is also characterized by the classic "hand-washing" stereotypic movements, irregular
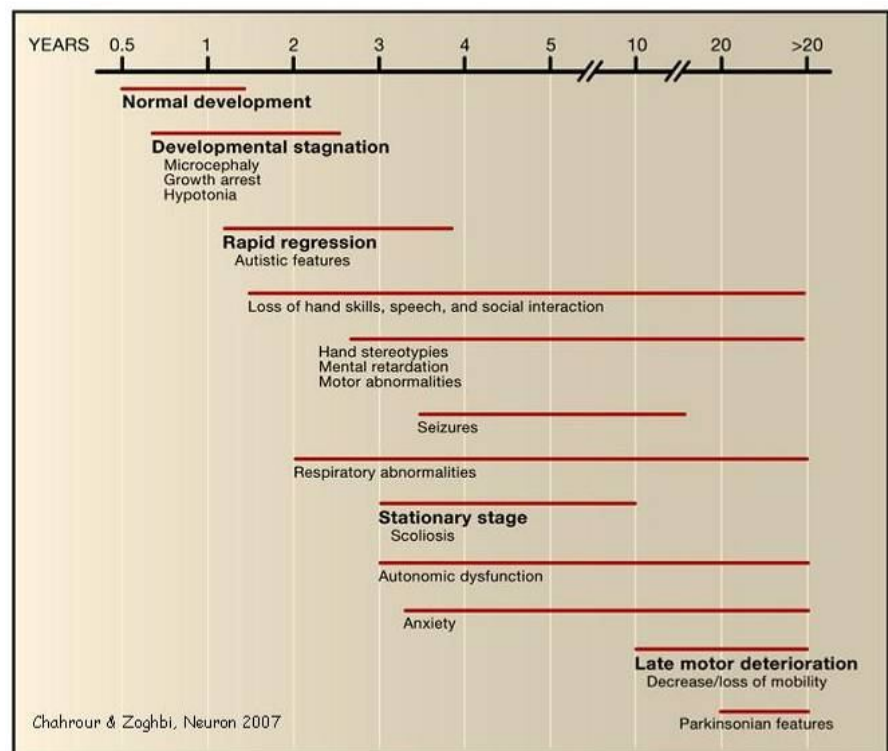
Figure 4: Time course of onset and progression of RTT clinical phenotypes. After a period of normal development, a healthy-looking baby girl falls into developmental stagnation, followed by rapid deterioration, loss of acquired speech, and the replacement of purposeful use of the hands with incessant stereotypies, a characteristic of the syndrome. Patients also develop social behaviour abnormalities and are often misdiagnosed as having autism. The condition worsens with loss of motor skills and profound cognitive impairment. In addition, patients suffer from anxiety, seizures, and a host of autonomic abnormalities. The scheme was taken from Chahrour & Zoghbi, 2007 [4].

breathing patterns, truncal and gait ataxia/apraxia; about half of patients also develop seizures. In Stage III (4-7 years), girls become more alert and interested both in people and their surrounding; however inability to speak, hand apraxia and the stereotypic hand activities persist. Other somatic and neurological handicaps, such as severe scoliosis, reduced somatic growth and epilepsy, become evident. Stage IV (5-15 years and older), is characterized by further somatic and neurological deterioration resulting in end-stage spastic quadriparesis.

In addition to typical RTT, it has been recognized that some individuals present many of RTT clinical features, such as regression, but do not necessarily have all of the features and disorders. These cases have been indicated as "variant" or "atypical" RTT and have been found to cluster in some distinct clinical grouping [32]. In particular, five distinct categories have been delineated on the basis of clinical criteria: i) the early-onset seizures variant, with seizures onset before regression; ii) the "forme fruste", characterized by a milder and incomplete clinical course (regression between 1 and 3 years); iii) the congenital variant, in which affected girls appear floppy and retarded since the very first months of life lacking the normal perinatal period typical of classic RTT; iv) the late regression variant which is rare and still controversial; v) the Zappella variant (previously known as Preserved Speech Variant; PSV), in which girls recover the ability to speech few words and third person phrases and display and improvement of purposeful hand movements at Stage 3 of disease progression. In addition to those outlined above, another variant has been described: the "highly functioning PSV", in which patients acquire the ability to express themselves using more complex language function including use of first person phrases [33]. Moreover, girls develop a better control of their hands and they are able to draw figures and write simple words. The degree of mental retardation in these girls is also milder than in the Zappella variant and their I.Q. can be as high as 50 [34].

1.2 FOXG1 and the congenital variant of RTT

In 2005, Shoichet et al reported a female patient exhibiting a severe cognitive disability associated with complete agenesis of the corpus callosum and microcephaly with a balanced de novo translocation t(2;14)(p22;q12) that disrupts the Forkhead box G1 (*FOXG1*, MIM #164874) gene [35]. Later on, different groups, including our, identified and characterized by array-CGH analysis three 14q12 interstitial overlapping deletions in two girls with psychomotor retardation, epilepsy, microcephaly and unusual facial features resembling RTT phenotype (2.9 and 3.6 MB) (Fig. 5 CASE A and B) and in a 10-month-old male patient with

mental retardation, microcephaly, and facial dysmorphisms (3.6 Mb) (Fig. 5 CASE C) [36-38]. The identified common deleted region was gene poor including only two genes: *FOXG1* and *PRKD1*. A functional analysis of these two genes, suggested that *FOXG1* could be an interesting candidate gene, since it encodes for a brain-specific transcriptional repressor.
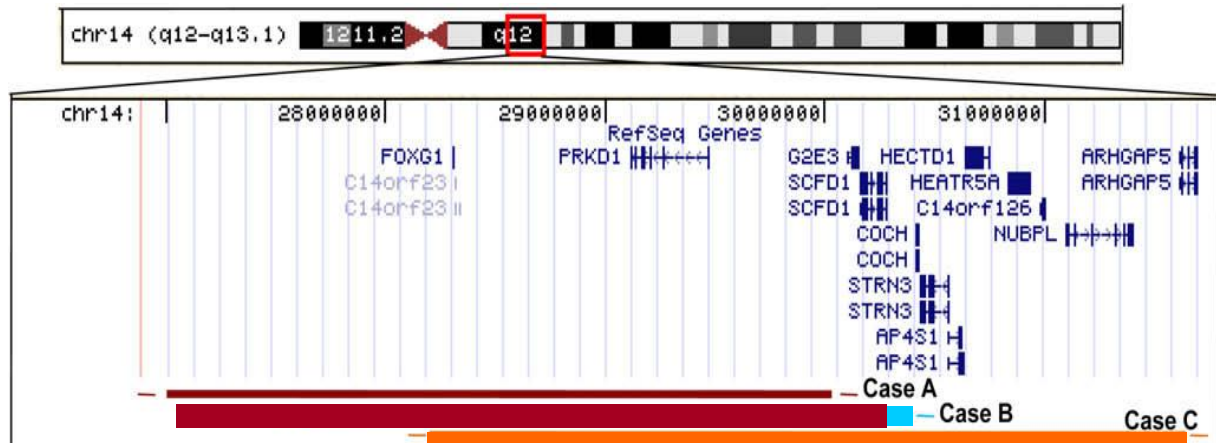
Figure 5: **USC Genome Browser Assembly view of chromosome 14** (http://genome.usc.edu). Chromosome 14 is represented in the upper panel. The red rectangle indicates the deleted region enlarged in the window below, which shows genes included in the rearrangement. Coloured bars indicate the extension of deletions identified in the 3 cases (A, B and C). The figure was taken from Mencarelli et al.2009 [38].

Mutation screening in a panel of *MECP2* mutation-negative RTT patients identified a *FOXG1*-null mutation in two congenital variant patients, indicating that *FOXG1* gene was indeed the cause of the most severe form of RTT, the congenital variant [31].

The congenital variant was first described by Rolando in 1985 [39]. In this condition, girls appear floppy, passive and easy to cry during the perinatal period. Girls show a deceleration of head growth and microcephaly is evident already before the fourth month of life and it is more severe than in classic RTT. Motor development is severely impaired and voluntary hand use is absent. Typical stereotypic hand movements with hand-washing and hand-mouthing activities are constant. Moreover, some patients present protruding tongue and jerky movements of the upper limbs, rarely present in classic RTT. Hypogenesis of the corpus callosum has been reveled in several patients [31,40].

Following the identification of the first 2 mutated patients, mutation screening of *FOXG1* in five small cohorts of patients with overlapping phenotype resulting negative for *MECP2* mutations identified 12 patients carrying intragenic mutations including five nonsense, four frameshift, and three missense mutations [31,40-43]. These patients exhibit features overlapping Rett phenotype although the significant difference is represented by the absence of the normal early development period.

In a very recent study, Kortum and colleagues performed an extensive clinical evaluation of *FOXG1* mutated patients and evidenced several clinical features that allow a phenotypic overlap with other complex developmental disorders beyond Rett syndrome. They indicated the presence of true dyskinesias and brain imaging abnormalities together with the lack of regression and of respiratory arrhythmia as the main features that do not overlap with Rett phenotype. Based on these findings, they asserted that the combination of a specific pattern of developmental features and brain malformations results in a specific clinically recognizable syndrome that they designated as "the *FOXG1* syndrome" [44].

1.2.1 The role of FoxG1 in the Telencephalon

FOXG1 gene encodes for a Fork-head box protein G1 (also referred to as Brain Factor 1; BF1) a transcription factor acting primarily as a transcriptional repressor through DNA binding. The main functional domains identified are: i) a fork-head domain allowing the protein to directly bind to DNA. ii) A JARID1B-binding domain through which the protein interacts with the transcriptional repressor *JARID1B* (Fig. 6).
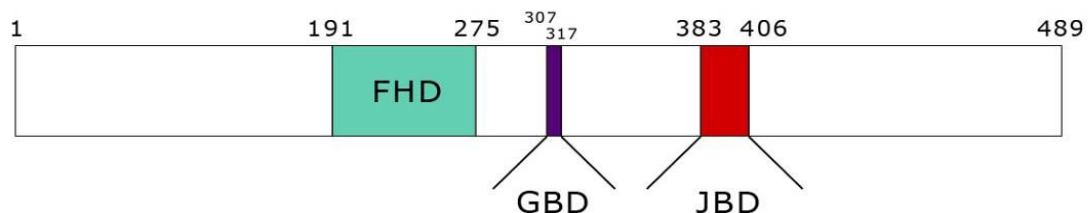
Figure 6: FoxG1 protein functional domains. The three main functional domains of FoxG1 protein are shown: the DNA binding fork-head domain in light blue (FHD), the Groucho-binding domain in violet (GBD) and the JARID1B binding domain in red (JBD). The numbers at the top refer to aminoacid positions.

JARID1B is a demethylase involved in the regulation of chromatin dynamics; it is capable of removing three methyl groups from histone H3 lysin 4 and it can regulate gene transcription alone or as part of a multiprotein complex that can include FoxG1. iii) A Groucho-binding domain that allows the interaction of FoxG1 with a global transcriptional co-repressor of the Groucho family that acts as both a corepressor and an adapter. Immunoprecipitation experiments evidenced that FoxG1 also indirectly interacts with the histone deacetylase 1 protein (HDAC1) forming a transcriptional repression complex [45].

Several studies in mice demonstrated that, during forebrain embryonic development, the expression of the mouse ortholog *Foxg1* is restricted to the central nervous system

coinciding with the emergence of the telencephalic structures. Its function has been extensively characterized demonstrating that *Foxg1* contributes to the development of telencephalon where it regulates the rate of neurogenesis by keeping progenitor cells in a proliferative state and by preventing their premature cortical differentiation [46-48]. *Foxg1* proliferative effects rely on its ability to inhibit the FoxO-Smad transcriptional complex and, therefore, to block p21Cip1 induction by TGF-beta signals in neuroepithelial cells. In fact, Smad proteins, activated by TGF-beta signaling, form a complex with FoxO proteins to turn on p21Cip1 gene. This gene in turn mediates cell cycle arrest at G1. The impasse of p21Cip1 activation by FoxG1 determines the release of this arrest and the subsequent cell cycle progression [49,50]. In accordance with this role in progenitors proliferation, *Foxg1* mutant brains show a remarkable reduction of the telencephalic vesicles due to a severely compromised growth of the telencephalon [51,52].

The telencephalon arises from the most rostral region of the neural tube and the anterior-posterior identity in the neuroaxis is determined by several intrinsic and extrinsic cellular factors that interact to set up the telencephalic domain during development. A primary role in the determination of dorsal and ventral telencephalic territories is performed by signaling molecules such as: Sonic hedgehog (SHH) and the zinc-finger transcription factor GLI-3 that specify ventral and dorsal domains, respectively; fibroblast growth factor 8 (FGF-8), essential for the generation of ventral cell types in the telencephalon; a paired box transcription factor 6 (PAX6), essential for the determination of dorsal regions by repressing ventral telencephalic gene expression; bone morphogenetic proteins (Bmps) and Wingless/Int proteins (WNTs) caudo-medially produced. These molecules are involved in specific signaling pathways that induce the activation of graded expression of transcription factors that in turn control the development of telencephalic cells, determining their molecular and cellular identities [52].

FoxG1 is one of the earliest transcription factors to be expressed in the part of the neural plate from which the telencephalon develops, playing a critical role in this process. In fact, FoxG1 probably coordinates the activity of the different signaling centers: it directly or indirectly regulates the expression of SHH, since Foxg1^{-/-} embryos have reduced telencephalic expression of this factor [52]. FoxG1 is also a key downstream effector of the Shh pathway during induction of ventral identity [53,54]. In addition, FoxG1 might regulate FGF-8 expression in rostral telencephalon during development, since Fgf8 expression is reduced in Foxg1^{-/-} embryos [55]. Moreover, despite its essential role in the ventral telencephalon, Foxg1 seems to be involved in the signaling pathway that induces the dorsal midline. In the dorsal

telencephalon, GLI-3 promotes the expression of bone morphogenetic proteins (BMPs) and Wingless/Int proteins (WNTs). FoxG1 inhibits Wnt/b-catenin signaling through direct transcriptional repression of Wnt ligands, thus restricting the dorsal Wnt signaling center to the roof plate and consequently limiting pallial identities. Therefore, FoxG1 absence results in a ventral expansion of roof plate Wnt and Bmp expression [56,57], correlated with increased Bmp activity inside the telencephalon [47,54,55,58]. Additional studies performed in Foxg1 KO mice revealed the absence of ventral telencephalic tissue, suggesting that Foxg1 also controls the formation of the compartment boundary between telencephalon and basal diencephalon. This is partially due to reduced production of the morphogens Shh and Fgf8, whose signaling is crucial for the specification of ventral telencephalic cell types. Even if Foxg1^{-/-} cells show some response to Shh and Fgf8 exposure, the expression of the ventral telencephalic marker genes is still absent. These data indicate that Foxg1 has a crucial cell-autonomous function, giving telencephalic cells the competence to develop ventral identities. In fact, experiments in chimeric embryos between Foxg1^{+/+} and Foxg1^{-/-} cells demonstrated that the cells lacking Foxg1 could contribute to ventral telencephalon, but they expressed dorsal rather than ventral telencephalic markers [53].

Recent studies in FoxG1^{+/-} heterozygous mice revealed that Foxg1, beyond its function during embryonic telencephalon development, plays a fundamental role in regulating adult dentate gyrus (DG) neurogenesis. Indeed, it is highly expressed in areas of postnatal neurogenesis, including the DG and the subventricular zone (SVZ) of the hippocampus. Its haploinsufficiency is responsible for impaired survival of postnatally-born DG neurons. As a consequence, Foxg1^{+/-} mice exhibit a marked reduction of DG size that progresses with age and they display behavioral and cognitive deficiencies consistent with hippocampal alterations [59,60].

The function of *FOXG1* in the developing human brain is presumably similar to that in the mouse. In particular, as in mice, *FOXG1* is strongly expressed in the neuroepitelium of the telencephalon and visual structure during development [44].

1.3 iPS and disease modeling

Most of our current knowledge about cellular phenotypes in neurodevelopmental and neurodegenerative diseases in human was gathered from studies in postmortem brain tissues. These tissues often represent the end-stage of the disease and therefore are not always a fair representation of how the disease developed [61]. In 2007 Takahashi et al reported a very

innovative technology based on genetic reprogramming of somatic cells to generate stem-like cells named induced Pluripotent Stem Cells (iPSCs) [62]. Takahashi and colleagues demonstrated that iPSCs can be generated through the retrovirus-mediated transfection of four transcription factors OCT-4, SOX-2, c-MYC and KLF-4 (Fig. 7) [63]. iPSCs are similar to human Embryonic Stem (hES) cells regarding gene expression profile, epigenetic marks and fate potential [64]. Like hES, they can be expanded indefinitely and differentiated *in vitro* into many different cell types [62]. Despite these similarities, iPSCs are not identical to hES cells and retain an epigenetic memory reflecting their tissue of origin [65]. iPSCs lines pass the most stringent tests of pluripotency, self-renewal, multi-lineage potential and, for mouse iPSCs, germline transmission (the ability to generate most mouse tissues after injection into an early embryo, including germ cells) [64,66]. Moreover, the injection of iPSCs in immuno-compromised mice induces the formation of teratomas containing derivatives of the three germ layers, a further proof of their pluripotency [64].

iPSCs represent a great opportunity to obtain humanized models for neurodevelopmental diseases, giving scientists a cellular tool for diseases phenotyping, drug screening and the development of personalized treatments. In fact, in the disorders of the nervous system the direct study of diseased tissue is limited by issues of accessibility and the inability of mature neurons to regenerate. The possibility to study diseased neural cells derived from iPSCs may provide breakthroughs for diagnosis and treatment of these disorders. In these last few years, iPSCs have been successfully derived from patients with both neurodegenerative (ALS, SMA, Parkinson, HD and FD) and neurodevelopmental (FRAXA, PW-AS) disorders and neuronal differentiation has been performed in some cases, using protocols developed for hESCs [61,67,68]. In particular, iPSCs from ALS and SMA patients have been successfully differentiated into motor neurons and glia cells confirming the potentiality of this system for establishing an *in vitro* diseases model with human living affected neurons [69,70].

Recently, Rett patients' iPSCs have been generated by different groups in order to investigate the molecular mechanisms of disease in neurons [71,72]. They derived iPSCs from *MECP2*-mutated patients fibroblasts and differentiated them into glutamatergic neurons. Phenotypic characterization of hiPSC cell-derived neurons from *MECP2*-mutated patients, revealed that these cells exhibit a significant reduction in soma size compared to control-derived neurons, confirming that neuronal maturation is severely affected in RTT. Moreover, Marchetto et al found that RTT neurons have a reduced number of dendritic spines compared to those derived from control iPSCs or hESCs. They also demonstrated an important

reduction in the frequency and amplitude of spontaneous excitatory and inhibitory postsynaptic currents in RTT neurons. It is important to underline that these findings are in accordance with data on mouse models and thus demonstrate the applicability of iPSCs technology to model RTT *in vitro* [71,72].
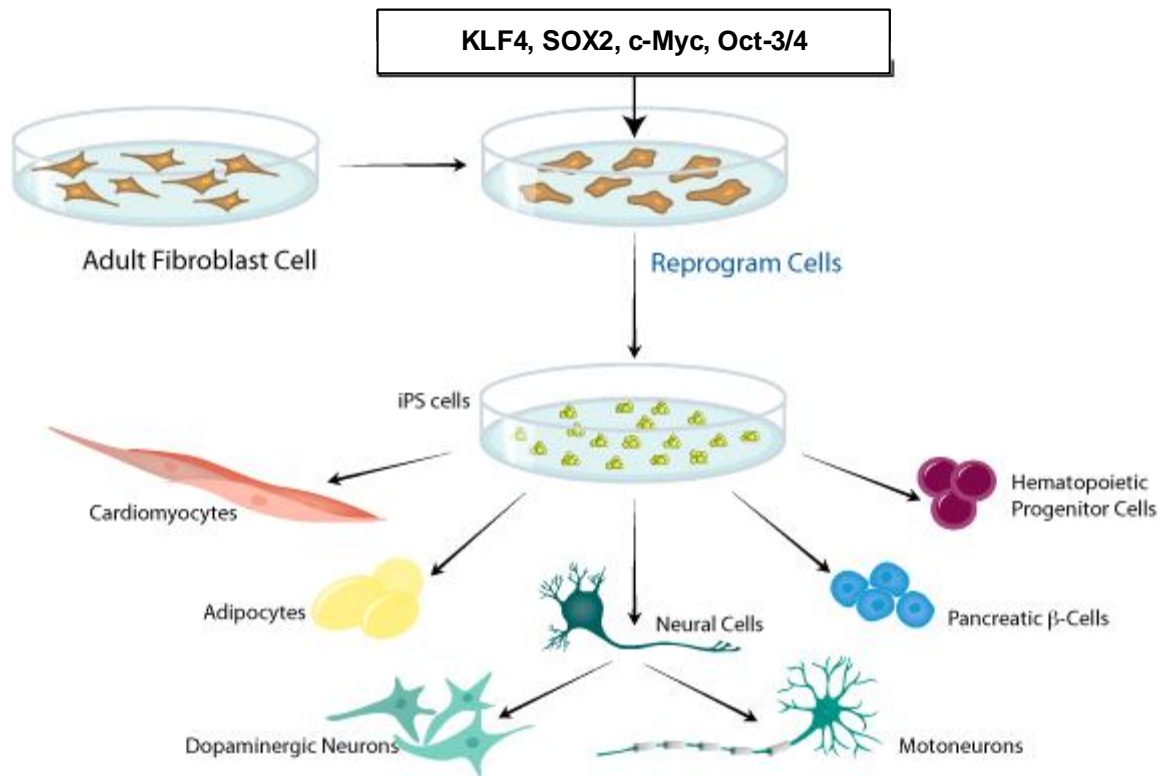
Figure 7: **Schematic view of iPSCs generation and cellular differentiation protocol.** iPS cells can be derived from adult somatic cells isolated from patients and controls through the introduction of the expression of exogenous transcription factors: KLF-4, SOX2, c-MYC and Oct-4. Using specific differentiation protocols, iPSCs can be then differentiated into different cellular types in vitro, recapitulating several defects found in patients and in animal models of the disease. The figure was taken from http://www.rndsystems.com

2. RATIONALE OF THE STUDY

One of the most common causes of mental retardation in females is represented by Rett Syndrome (RTT). It is a severe neurodevelopmental disorder characterized by an apparently normal period for the first 6-18 months of life, followed by the loss of cognitive capability and of psychomotor and acquired hand skills. The clinical characteristics usually associated with classical RTT patients include mental retardation, acquired microcephaly, autistic features, seizures, ataxia and "hand-washing" stereotypic movements. Beside the typical form of RTT due to *MECP2* mutations, other five variants have been identified based on their clinical signs ranging from milder phenotypes, with a later onset, to more severe manifestations. Among these, the congenital variant issues for the severity of its phenotype considering that the early normal period is absent and girls appear floppy and retarded since the very first months of life. In 2007, array-CGH analysis in patients with RTT-like phenotype allowed our group to identify the brain specific transcriptional repressor *FOXG1* as a possible candidate gene for RTT. Subsequently, the identification of *FOXG1*-null mutations in two congenital variant patients negative for *MECP2* mutations suggested the possible association between *FOXG1* and this variant. In order to confirm this hypothesis, during my first year of Ph.D. study, I performed the molecular analysis of *FOXG1* gene in mutation-negative RTT patients. To better clarify the clinical phenotype, the study was extended to an international cohort of patients, including also girls with a phenotype different from the congenital variant.

FoxG1 protein is dynamically involved in global chromatin regulation performing its function either alone or as a part of multiprotein complexes. At single cellular level, FoxG1 is localized to the nucleus, outside the heterochromatin foci, suggesting that its binding to chromatin is not static. So far, little is known about the relationship between FoxG1 and chromatin and its functional role in the nucleus. We thus decided to investigate this issue by performing studies aimed at clarifying the properties FoxG1 binding to chromatin *in vivo*.

During early neurodevelopment, FoxG1 is essential for the correct neurogenesis of the telencephalic progenitor cells. However, the protein is still expressed in post-natal tissues, suggesting that its function could be essential also in post-mitotic neurons. For this reason, the investigation of its role in these cells could allow to better define the molecular mechanisms that induce patient's phenotype. Up to now, studies on animal models have contributed to

understand neural development, but, considering the high complexity of the human brain, these models appear limitative so that the need of a human neural model comes out. Recently, consistent results in the study of neurodevelopmental disorders have been obtained by the application of iPS technology. During last year of my Ph.D. course, I thus focused on the set up of a reprogramming protocol in order to obtain iPS cells starting from fibroblasts isolated from *FOXG1*-mutated patients having the final aim to differentiate them into neurons. This approach represents the innovative opportunity to obtain *in vitro* affected neurons from a specific individual bypassing all legal and ethic limitations. Moreover, this approach open the way to future patient-specific drug screenings, since generated neural cells maintain the genetic identity of the person of origin.

Despite several efforts to understand FoxG1 molecular function, only few target genes including p27Xic in Xenopus and p21Cip, Bmp4 and Fgf8 in mouse have been identified through functional studies based on a candidate gene approach. [50,55,58,73]. To identify additional target of this transcriptional regulator, we thus decided to perform expression profiling studies in *Foxg1* deficient mouse brain in order to identify interesting *FOXG1* target genes and thus define the molecular pathways altered during neural maturation as a consequence of its absence.

Novel *FOXG1* mutations associated with the congenital variant of Rett syndrome

M A Mencarelli,[1] A Spanhol-Rosseto,[1] R Artuso,[1] D Rondinella,[1] R De Filippis,[1] N Bahi-Buisson,[2] J Nectoux,[2] R Rubinsztajn,[2] T Bienvenu,[2] A Moncla,[3] B Chabrol,[3] L Villard,[4] Z Krumina,[5] J Armstrong,[6] A Roche,[6] M Pineda,[6] E Gak,[7] F Mari,[1] F Ariani,[1] A Renieri[1]

[1]Medical Genetics, Department of Molecular Biology, University of Siena, Siena, Italy [2]Université Paris Descartes, Institut Cochin, Inserm U567, Paris, France [3]Inserm U910, Université de la Méditerranée, Assistance Publique Hôpitaux de Marseille, Hôpital de La Timone, Marseille, France [4]Inserm U910, Université de la Méditerranée, Faculté de Médecine de La Timone, Marseille, France [5]Medical Genetics Clinic of Latvian State, Children's University Hospital, Latvia [6]Hospital Sant Joan de Déu, Esplugues, Barcelona, Spain [7]Sagol Neuroscience Center, Sheba Medical Center, Tel Hashomer affiliated to the Sackler School of Medicine, Tel Aviv University, Tel Aviv, Israel

Correspondence to
Alessandra Renieri, Medical Genetics, Molecular Biology Department, University of Siena, Viale Bracci, 2, 53100 Siena, Italy; renieri@unisi.it

Received 16 March 2009
Revised 21 May 2009
Accepted 30 May 2009
Published Online First
2 June 2009

ABSTRACT

Background Rett syndrome is a severe neurodevelopmental disorder representing one of the most common genetic causes of mental retardation in girls. The classic form is caused by *MECP2* mutations. In two patients affected by the congenital variant of Rett we have recently identified mutations in the *FOXG1* gene encoding a brain specific transcriptional repressor, essential for early development of the telencephalon.

Methods 60 *MECP2/CDKL5* mutation negative European Rett patients (classic and variants), 43 patients with encephalopathy with early onset seizures, and four atypical Rett patients were analysed for mutations in *FOXG1*.

Results and conclusions Mutations have been identified in four patients, independently classified as congenital Rett variants from France, Spain and Latvia. Clinical data have been compared with the two previously reported patients with mutations in *FOXG1*. In all cases hypotonia, irresponsiveness and irritability were present in the neonatal period. At birth, head circumference was normal while a deceleration of growth was recognised soon afterwards, leading to severe microcephaly. Motor development was severely impaired and voluntary hand use was absent. In contrast with classic Rett, patients showed poor eye contact. Typical stereotypic hand movements with hand washing and hand mouthing activities were present continuously. Some patients showed abnormal movements of the tongue and jerky movements of the limbs. Brain magnetic resonance imaging showed corpus callosum hypoplasia in most cases, while epilepsy was a variable sign. Scoliosis was present and severe in the older patients. Neurovegetative symptoms typical of Rett were frequently present.

INTRODUCTION

Rett syndrome (RTT) is characterised by a serious and global developmental disorder affecting the central nervous system. First described by Andreas Rett 40 years ago, the syndrome has been the object of extensive investigations, revealing a wide spectrum of clinical phenotypes including the classic form, the early onset seizure variant, the Zappella variant (Z-RTT), the congenital variant, the 'forme fruste' variant, and the late regression variant.[1–3] Mutations in the *MECP2* gene, located in Xq28, are responsible for 95% of classic RTT and for 50% of Z-RTT[4]; while the early onset seizure variant results from mutations in the *CDKL5* gene, in Xp22.[5] We have recently used a candidate gene approach to demonstrate that the *FOXG1* gene, located in 14q12, is responsible for the congenital variant of RTT.[3] In this variant, initially described by Rolando in 1985, the affected girls present the same clinical features as in classic RTT, but in addition they are floppy and retarded from the very first months of life.[6]

We report the identification of *FOXG1* mutations in four additional congenital RTT girls, through mutation screening of a cohort of 107 European patients: 60 RTT patients (classic and variants), 43 patients with epileptic encephalopathy, and four RTT-like patients. Clinical data of these four patients were compared with the two previously reported girls in order to improve the characterisation of the phenotype associated with *FOXG1* mutations.[3]

PATIENTS AND METHODS
Patients and phenotype definitions

We collected a cohort of 107 European patients (56 patients from France, 49 from Spain and 2 from Latvia) with the following clinical classification: 60 RTT girls (33 classic, 16 congenital, 7 with early onset seizures, 2 late regression, 1 Z-RTT and 1 'forme fruste'), 43 patients with encephalopathy with early onset seizures (40 females and 3 males), and 4 RTT-like patients (1 female and 3 males with microcephaly, hand stereotypies and autistic features). Patients with classic and variant RTT were diagnosed according to the international criteria.[7] RTT-like cases are patients who show some RTT clinical features but who do not fulfil all diagnostic criteria for classic or variant RTT. Phenotypic scores have been calculated using the severity score system previously reported by Renieri et al.[2] All patients have been tested negative for *MECP2* and *CDKL5* mutations by a combination of denaturing high performance liquid chromatography (DHPLC) and multiplex ligation dependent probe amplification/quantitative polymerase chain reaction (MLPA/qPCR) analysis.

Molecular analysis

Blood samples were obtained after informed consent. DNA was extracted from peripheral blood using a QIAamp DNA Blood Kit (Qiagen GmbH QIAGEN strasse 1, 40724 Hilden, Germany). To determine the appropriate DNA concentration, we used the OD260/280 method on a photometer.[8] DNA samples were screened for mutations in *FOXG1* gene using Transgenomic WAVE DHPLC. The entire

coding portion of *FOXG1* was analysed as previously reported.[3] PCR products resulting in abnormal DHPLC profiles were sequenced on both strands using PCR primers with fluorescent dye terminators on an ABI PRISM 310 genetic analyser (PE Applied Biosystems, Foster City, California, USA).

Clinical score

For each patient a severity score was assigned through the evaluation of 22 different clinical signs.[2] Results were compared with the severity score of 128 classic and 25 Z-RTT patients with mutation in the *MECP2* gene, and nine patients with the early onset seizures variant of RTT with a *CDKL5* mutation.[2 9] Statistical analysis was performed using the median test.

RESULTS
Molecular analysis

A mutation in the *FOXG1* gene was identified in four patients clinically classified as congenital RTT. The *de novo* origin of the mutation was confirmed in three cases (cases 2—4), while in one case (case 1) parents were not available. Cases 3 and 4 bear the truncating mutations p. S185fsX454 (c.551_552insC) and p.Y208X (c.624C>G). The remaining two cases have missense mutations that lie within the forkhead domain and affect residues highly conserved in different species (including *Tetraodon nigroviridis*—CAF93027; *Xenopus tropicalis*—NN_001116933; and *Xenopus laevis*—NP_001079165): p.N227K (c.681C>G) in case 1 and p.F215L (c.643T>C) in case 2.

Clinical description

Case 1 (1091) is a female from Latvia, presently aged 17 years; she is in the fourth stage of RTT with spastic paraparesis (table 1; figure 1B). Since the age of 16 months she has grown up in an orphanage and her parents are presently unavailable. The girl was her mother's first child and was born after a normal pregnancy. Birth weight was 3900 g with an Apgar score 8/9. Psychomotor delay was appreciated from the age of 6—7 months. The time of occurrence of the first seizures is unknown. The girl has been examined only once, at the age of 13 years 2 months.

Case 2 (RTT00967) is a female from France, presently aged 8 years 6 months (table 1, figure 1C). She is the second child of a non-consanguineous couple; another child was born afterwards. She was born at 39 weeks after a normal pregnancy. Auxological parameters at birth were normal. In the neonatal period sleep disturbance and severe distress (crying) were noticed. She was referred to a clinical unit at 6 months because of psychomotor retardation. At this age, examination revealed severe hypotonia with sleep disturbances and no dysmorphic features except strabismus and hypermetropia. A re-evaluation at 2 years showed normal weight and height (height 81 cm, weight 12 kg), while the occipitofrontal circumference (OFC) was at −2 SD (45 cm), with developmental delay, hypotonia, very poor social contact, manual stereotypies and dystonia of the extremities. At 6.5 years, she could only stand up with support and did not walk; could hold an object (feeding bottle) with a simple grasp; and showed trunk rocking and tongue chewing. On last examination, at 8 years of age, the clinical phenotype was unchanged; she was only able to pronounce two disyllabic words (mama, papa) and brain magnetic resonance imaging (MRI) showed microcephaly with abnormal development of the frontal lobes without gyration defect.

Case 3 (RTT01158) is a female from France, presently aged 3 years (table 1). The patient is the first child of non-consanguineous parents from Benin, without a relevant family history. She was born at term and showed normal auxological parame-

ters. She developed severe microcephaly at an early stage. Brain MRI performed in the first months showed isolated ventricular dilatation. Subsequently, she developed severe epileptic encephalopathy. In addition she had a disturbed sleep pattern from 2 years. When last examined, she was able to hold her head steadily but showed asymmetric spastic tetraplegia and scoliosis. Brain MRI performed at 2 years showed delayed myelination with hypoplasia/hypomyelination of the corpus callosum.

Case 4 (60719368) is a female from Spain, presently aged 3 years 2 months (table 1, figure 1A). The mother has a normal boy of 9 years and has had three spontaneous abortions. At birth she showed very severe hypotonia and normal auxological parameters. Subsequently microcephaly became evident. At 4 months OFC was at −2SD, at 9 months at −3.5, and since the age of 2 years at −5SD. She developed hand stereotypies at 12 months: she used to bring her hands to the mouth and pat her fingers on her lips. Protruding tongue movements have been constant from the age of 4 months.

Clinical comparison of the six patients with *FOXG1* mutations

We compared the clinical picture of these four additional patients with a *FOXG1* mutation to the two previously reported.[3] These six patients, with age ranging from 3—22 years, present a distinct clinical phenotype (table 1).

In order to recognise the clinical differences among the RTT phenotypes, we compared the clinical scores of four patients with mutations in *FOXG1* for whom we could obtain complete clinical information (patients 3—6) to the scores of classic and Z-RTT patients with *MECP2* mutations and those of early onset seizure variant patients with *CDKL5* mutations. In patients with a *FOXG1* mutation the clinical score median value is 31.5, with total score ranging from 28—38. Among the classic RTT cases the median value is 27, with a range from 13—39.[9] In the nine patients with *CDKL5* mutation, the median value is 27, with total score ranging from 22—30.[9] In the Z-RTT the median value is 13, with values ranging from 4—24.[2]

DISCUSSION

This work confirms that the *FOXG1* gene is responsible for the congenital variant of RTT. In fact, *FOXG1* mutations (figure 2) have so far been identified only in patients originally classified by different clinical centres as affected by this variant of RTT.

The overall clinical phenotype is characterised by normal pregnancy and delivery, normal auxological parameters at birth, followed by hypotonia, irresponsiveness and irritability in the neonatal period. Deceleration of head growth represents one of the most important diagnostic signs: in the four cases for whom the OFC had been recorded in the first months of life, microcephaly was evident already before the fourth month. Apparently microcephaly is more severe than in classic RTT (mean −4.32 SD compared with a mean of −2.4 SD in classic RTT). All five patients bearing a rearrangement on chromosome 14q12 involving *FOXG1* presented with microcephaly: in the first reported case the onset was not defined[10]; in three patients microcephaly was evident between 5—8 months[11—13]; while in the fifth patient head circumference was below the third centile at the age of 11 months.[14]

In the two girls previously described with *FOXG1* mutations, a retrospective assessment as to whether there had been a period of normal development was not feasible, although the parents noted a delay only at 3 months. In patient 3, who presented with the earliest onset, a real regression period was not identifiable, while the other three cases (patients 1, 2 and 4) presented a regression before 6 months of age, more precocious than in classic RTT, in

24

Table 1 Clinical features of patients with *FOXG1* mutations

	Patient 1 (1091)	Score	Patient 2 (RTT00967)	Score	Patient 3 (RTT01158)	Score	Patient 4 (60718368)	Score	Patient 5 Ariani *et al*[3]	Score	Patient 6 Ariani *et al*[3]	Score
Age/sex	13 y 2 m/female		8 y/female		3 y/female		3 y 2 m/female		22 y/female		7 y/female	
Inheritance	Parents not available (NA)		De novo		Parents' DNA requested		De novo		De novo		De novo	
Mutation	c.681C>G; p.N227K		c.643T>C; p.F215L		c.551_552insC; p.S185fsX454		c.624C>G; p.Y208X		c.765G>A; p.W255X		c.969delC; p.S323fsX325	
OFC at birth	NA		34 cm 50—75th cnt		32.5 cm 3—10th cnt		33.5 cm 25—50th cnt		34 cm 50th cnt		34 cm 50th cnt	
Weight at birth	3900 g 90th cnt		3300 g 50—75th cnt		2800 g 10th cnt		3150 g 50th cnt		3150 g 25—50th cnt		3350 g 50th cnt	
Length at birth	NA		49 cm 50th cnt		48 cm 50th cnt		50 cm 50th cnt		49 cm 50th cnt		50 cm 50th cnt	
Perinatal signs	NA		Inconsolable crying		Hypotonia, psychomotor retardation		Sleepiness, cries only if hungry		Inconsolable crying		Inconsolable crying	
Age of regression	6 months	2	6 months	2	3 months	2	3 months	2	3 months	2	3 months	2
Present OFC	46 cm −6 SD	2	48 cm −2.24 SD	2	43 cm −5 SD	2	42 cm −5 SD	2	49 cm −4 SD	2	47 cm −3.7 SD	2
Present weight	NA		NA		13.4 kg 3rd cnt	1	10 kg <5th cnt	2	38 kg <5th cnt BMI 19.1	2	18.5 kg <5th cnt BMI 15.3	2
Present height	NA		NA		97 cm 75th cnt	0	87 cm <3rd cnt	2	141 cm <<5th cnt	2	110 cm <5th cnt	2
Hand stereotypy	NA		Intermittent: hand to mouth, washing	1	Intermittent	1	Constant: hand to mouth	2	Constant: clapping, hand to mouth	1	Constant: clapping, hand to mouth	2
Age of stereotypy onset	NA		NA		NA		12 months		NA		12 months	
Jerky movements	NA		Yes		Yes		Occasional		Yes		Yes	
Rocking	Yes		NA		Absent		No		Yes		No	
Voluntary hand use	NA		Poor	1	Absent	2	Poor	1	Absent	2	Absent	2
Sitting	NA		15 months	0	Not acquired	2	No sitting alone	2	Not acquired	2	10 months	1
Walking	Not acquired	2	Not acquired	2	Not acquired	2	Not acquired	2	Not acquired	2	Not acquired	2
Age at walk	Never		Never	2	Never	2	Never	2	Never	2	Never	2
Speech	Not acquired	2	Not acquired	2	Not acquired	2	Not acquired	2	Not acquired	2	Not acquired	2
Age of increasing words	Never	2	Never	2	Never	2	Never	2	Never	2	Never	2
Level of speech	Absent	2	Absent	2	Absent	2	Absent	2	Absent	2	Absent	2
Level of phrases	Absent	2	Absent	2	Absent	2	Absent	2	Absent	2	Absent	2
Epilepsy	Not controlled by therapy	2	No epilepsy	0	Recurrent status epilepticus controlled by treatment	1	No epilepsy (3 years)	0	Not controlled by therapy	2	Controlled by therapy	1
Seizure onset	NA		Never		17 months		Never (3 years)		14 years		30 months	
Sleep disturbances	NA		Yes		Yes, severe		No		Yes		Yes	
Eye contact	NA		Poor		Poor		Good at 12 months		Poor		Poor	
Gastro-intestinal disturbances	NA		Moderate constipation	1	Severe, reflux and constipation	2	Constipation	1	Constipation	1	Constipation	1
Breathing disorders	NA		No	0	No	0	Apnoeas	1	Sporadic hyperventilation episodes	1	Prolonged inspirations	1
Cold extremities	NA		Yes	1	No	0	No	0	Mild	1	Mild	1
Tongue protruding movements	NA		Yes		No		Yes		Yes		Yes	
Bruxism	Yes		No		Yes		Yes, teeth chattering		Yes		Teeth beating/teeth-chattering	
Sialorrhea	NA		No		Yes		Yes		Yes		Yes	
Pain threshold	NA		Normal		Normal		High				High	
Joint rigidity	NA		No		No		No		Yes, large and small joints		Small joints	
Strabismus	NA		Yes		Yes		Yes		Yes		Yes	
Sphincter control	NA		No	2	Absent	2	Absent	2	Absent	2	Absent	2
Genu valgu	NA		NA		No	0	Absent		Severe	2	Absent	0
Pes planus	NA		Absent	0	NA		Mild	1	NA		NA	

25

Table 1 Continued

	Patient 1 (1091)	Score	Patient 2 (RTT00967)	Score	Patient 3 (RTT01158)	Score	Patient 4 (60718368)	Score	Patient 5 Ariani et al[3]	Score	Patient 6 Ariani et al[3]	Score
Scoliosis	Severe	2	No	0	No	0	Absent	0	Severe	2	Absent	0
Kyphosis	NA		No	0	Yes	1	Severe	2	Severe	2	Absent	0
Corpus callosum thinning at brain MRI	NA		No		Yes		Yes		Yes, mild		Yes, mild	
Total score	—		—			28		32		38		31

accordance with the diagnosis of the congenital variant. Motor development is severely impaired: no girl with a mutation could either walk with support or speak, although cases 2 and 6 can stand up with assistance (figure 1C). Voluntary hand use was absent in the majority of patients (3/5) and poor in two (cases 2 and 4). Poor eye contact and absence of response to social interaction were evident in five out of six patients, in contrast with classic RTT where eye contact is intense, and this feature represents a supportive criterion for diagnosis.

Stereotypic hand movements are typical as in classic RTT, with intense and continuous hand washing and hand mouthing activities. In addition, all girls showed constant thrusting of the tongue. These repetitive movements are not so typical of classic RTT, where ineffective chewing movements (seen in one of our patients) are found rather than thrusting of the tongue. Similar tongue protruding movements were present in the girl with the 14q12 deletion, which led to the identification of *FOXG1* mutations in the first patients with congenital RTT.[12] Also, in 4/5 patients jerky movements are often seen in the upper limbs, that are frequently pushed in different directions, while in classic RTT such movements are rarely reported.

In this small cohort of patients, epilepsy was a variable sign: two girls, aged 3 years and 6.5 years respectively, have never presented with epileptic seizures (cases 2 and 4); in four patients epilepsy was present with an onset between 14 and 30 months. In two the epilepsy was well controlled by antiepileptic drugs (patients 3 and 6), while in the remaining two, seizures recurred despite treatment.

Neurological and neurovegetative symptoms are consistent with a diagnosis of RTT: constipation is reported in 4/6 patients; breathing abnormalities in 4/6; cold extremities in 3/6; bruxism in 4/6; sialorrhea in 4/6. Skeletal alterations such as scoliosis and kyphosis, genu valgu and pes planus are severe in the older cases.

Brain MRI showed corpus callosum hypoplasia in four patients, and this has been excluded in only one of the remaining two cases. Moreover, complete agenesis of the corpus callosum has been identified in patients with chromosomal rearrangements involving *FOXG1*.[11 15] All these findings are in accord with the phenotype of heterozygous *Foxg1*^{+/−} mice, showing a corpus callosum defect.[3]

Our results contribute to the clarification of the phenotype associated with *FOXG1*, confirming its role in the RTT spectrum. In particular, they seem to be associated with the most severe end of this spectrum. In fact, the median of the total clinical score in this group of patients is higher in comparison with patients affected by classic or early onset seizure variant of RTT.

All the patients reported to date with *FOXG1* mutations are female. This is probably due to an ascertainment bias and we expect that further mutations will be identified in male cases, given that *FOXG1* is an autosomal gene.

In conclusion, we suggest that *FOXG1* gene mutation analysis should be performed in female and male patients showing RTT features but lacking the typical early normal period due to the

Figure 1 Pictures of three of the new patients with *FOXG1* mutations. Panel A, case 4; panel B, case 1; panel C, case 2. Note in patient 4 the constant and intense hand to mouth stereotypic activities. The severe microcephaly of case 1 is clearly evident. Patient 2, presently aged 6 years 6 months, is able to stand up only with support but she cannot walk. Parental/guardian consent has been obtained.

26

Figure 2 *FOXG1* mutations and alterations of the functional domains. Schematic representation of FoxG1 protein. The three main functional domains are shown: the DNA binding fork-head domain, the Groucho binding domain and the JARID1B binding domain is red. The numbers at the top refer to the amino acid positions. The frameshift and stop mutations are showed below by zigzag lines. The missense mutations are indicated at the top. The asterisks indicate the two mutations previously reported in Ariani *et al.*[3]

---

precocious onset of symptoms. Besides other features typical of classic RTT, major signs possibly indicating a *FOXG1* mutation are severe psychomotor delay with inability to walk, severe postnatal microcephaly evident before the age of 4 months, poor eye contact, tongue stereotypies, jerky movements of limbs, and corpus callosum hypoplasia.

REFERENCES

1. **Chahrour M**, Zoghbi HY. The story of Rett syndrome: from clinic to neurobiology. *Neuron* 2007;**56**:422—37.
2. **Renieri A**, Mari F, Mencarelli MA, Scala E, Ariani F, Longo I, Meloni I, Cevenini G, Pini G, Hayek G, Zappella M. Diagnostic criteria for the Zappella variant of Rett syndrome (the preserved speech variant). *Brain Dev* 2009;**31**:208—16.
3. **Ariani F**, Hayek G, Rondinella D, Artuso R, Mencarelli MA, Spanhol-Rosseto A, Pollazzon M, Buoni S, Spiga O, Ricciardi S, Meloni I, Longo I, Mari F, Broccoli V, Zappella M, Renieri A. FOXG1 is responsible for the congenital variant of Rett syndrome. *Am J Hum Genet* 2008;**83**:89—93.
4. **Scala E**, Longo I, Ottimo F, Speciale C, Sampieri K, Katzaki E, Artuso R, Mencarelli MA, D'Ambrogio T, Vonella G, Zappella M, Hayek G, Battaglia A, Mari F, Renieri A, Ariani F. MECP2 deletions and genotype-phenotype correlation in Rett syndrome. *Am J Med Genet A* 2007;**143**:2775—84.
5. **Mari F**, Azimonti S, Bertani I, Bolognese F, Colombo E, Caselli R, Scala E, Longo I, Grosso S, Pescucci C, Ariani F, Hayek G, Balestri P, Bergo A, Badaracco G, Zappella M, Broccoli V, Renieri A, Kilstrup-Nielsen C, Landsberger N. CDKL5 belongs to the same molecular pathway of MeCP2 and it is responsible for the early-onset seizure variant of Rett syndrome. *Hum Mol Genet* 2005;**14**:1935—46.
6. **Rolando S**. Rett syndrome: report of eight cases. *Brain Dev* 1985;**7**:290—296.
7. **Hagberg B**, Hanefeld F, Percy A, Skjeldal O. An update on clinically applicable diagnostic criteria in Rett syndrome. Comments to Rett Syndrome Clinical Criteria Consensus Panel Satellite to European Paediatric Neurology Society Meeting, Baden Baden, Germany, 11 September 2001. *Eur J Paediatr Neurol* 2002;**6**:293—7.
8. **Sambrook J**, Fritsch EF, Maniatis T. *Molecular cloning: a laboratory manual*. 2nd edn. Cold Spring Harbor Laboratory Press, Woodbury, New York, USA. 1989.
9. **Artuso R**, Mencarelli MA, Polli R, Sartori S, Ariani F, Pollazzon M, Marozza A, Cilio MR, Specchio N, Vigevano F, Vecchi M, Boniver C, Bernardina BD, Parmeggiani A, Buoni S, Hayek G, Mari F, Renieri A, Murgia A. Early-onset seizure variant of Rett syndrome: definition of the clinical diagnostic criteria. *Brain Dev* Published Online First: 2009 doi:10.1016/j.braindev.2009.02.004.
10. **Grammatico P**, de Sanctis S, di Rosa C, Cupilari F, del Porto G. First case of deletion 14q11.2q13: clinical phenotype. *Ann Genet* 1994;**37**:30—2.
11. **Shoichet SA**, Kunde SA, Viertel P, Schell-Apacik C, von Voss H, Tommerup N, Ropers HH, Kalscheuer VM. Haploinsufficiency of novel FOXG1B variants in a patient with severe mental retardation, brain malformations and microcephaly. *Hum Genet* 2005;**117**:536—44.
12. **Papa FT**, Mencarelli MA, Caselli R, Katzaki E, Sampieri K, Meloni I, Ariani F, Longo I, Maggio A, Balestri P, Grosso S, Farnetani MA, Berardi R, Mari F, Renieri A. A 3 Mb deletion in 14q12 causes severe mental retardation, mild facial dysmorphisms and Rett-like features. *Am J Med Genet A* 2008;**146A**:1994—8.
13. **Mencarelli MA**, Kleefstra T, Katzaki E, Papa FT, Cohen M, Pfundt R, Ariani F, Meloni I, Mari F, Renieri A. 14q12 Microdeletion syndrome and congenital variant of Rett syndrome. *Eur J Med Genet* 2009;**52**:148—52.
14. **Bisgaard AM**, Kirchhoff M, Tumer Z, Jepsen B, Brondum-Nielsen K, Cohen M, Hamborg-Petersen B, Bryndorf T, Tommerup N, Skovby F. Additional chromosomal abnormalities in patients with a previously detected abnormal karyotype, mental retardation, and dysmorphic features. *Am J Med Genet A* 2006;**140**:2180—7.
15. **Schuffenhauer S**, Leifheit HJ, Lichtner P, Peters H, Murken J, Emmerich P. De novo deletion (14)(q11.2q13) including PAX9: clinical and molecular findings. *J Med Genet* 1999;**36**:233—6.

27

Expanding the phenotype associated with *FOXG1* mutations and in vivo FoxG1 chromatin-binding dynamics.

De Filippis R1*, Pancrazi L2,3*, Bjørgo K4, Rosseto A1, Kleefstra T5, Grillo E1, Panighini A2, Meloni I1, Ariani F1, Mencarelli MA1, Hayek J6, Renieri A1^, Costa M2^, Mari F1.
*both authors contributed equally to the work
^corresponding authors

1 Medical Genetics, Dept. Molecular Biology, University of Siena, Italy.
2 Institute of Neuroscience, Italian National Research Council (CNR), Pisa, Italy.
3 Scuola Normale Superiore, Pisa, Italy.
4 Department of Medical Genetics, Oslo University Hospital, Norway.
5 Department of Human Genetics, Radboud University Nijmegen, Netherlands.
6 Child Neuropsychiatry University Hospital AOUS Siena, Italy.

Corresponding authors:

Alessandra Renieri, Medical Genetics
University of Siena-Policlinico Le Scotte
Viale Bracci, 2 – 53100 Siena – Italy
E-mail: renieri@unisi.it
Phone: +390577233303; Fax +390577233325

Mario Costa
Institute of Neuroscience, Italian
National Research Council (CNR)
mario.costa@in.cnr.it
Phone: +390503153200

This manuscript was submitted to Clinical Genetics accepted with revisions.

Abstract

Mutations in the Forkhead box G1 (*FOXG1*) gene, a brain specific transcriptional factor, are responsible for the congenital variant of Rett Syndrome. Until now *FOXG1* point mutations have been reported in 12 Rett patients. Recently 7 additional patients have been reported with a quite homogeneous severe phenotype designated as the *FOXG1* syndrome. Here we describe two unrelated patients with a de novo *FOXG1* point mutation, p.Gln46X and p.Tyr400X respectively, having a milder phenotype and sharing a distinctive facial appearance. Although FoxG1 action depends critically on its binding to chromatin, very little is known about the dynamics of this process. Using fluorescence recovery after photobleaching, we demonstrated that most of the GFP-FoxG1 fusion protein associates reversibly to chromatin whereas the remaining fraction is bound irreversibly. Furthermore, we showed that the two pathologic derivatives of FoxG1 described in this paper present a dramatic alteration in chromatin affinity and irreversibly bound fraction in comparison with Ser323fsX325 mutant (associated with a severe phenotype) and wild type Foxg1 protein. Our observations suggest that alterations in the kinetics of FoxG1 binding to chromatin might contribute to the pathological effects of *FOXG1* mutations.

Introduction

Rett Syndrome (RTT; OMIM#312750) is a neurodevelopmental disorder that represents one of the most common causes of intellectual disability in girls. It is characterized by high clinical variability revealing a wide spectrum of phenotypes. Besides the classic form associated with *MECP2* (OMIM#300005) mutations, three other variants have been associated with a specific molecular defect (1). They include the Zappella variant (Z-RTT) due to *MECP2* mutations, the early-onset seizure variant, mostly due to *CDKL5* (OMIM#300203) mutations and the congenital variant, associated with *FOXG1* (OMIM#164874) mutations (1). Genotype-phenotype associations can be variable and *MECP2*-mutated early onset seizure variant cases and congenital variant cases can be occasionally found (2-4). At the same time a *FOXG1* mutation has been identified in one patient with a classic phenotype (5). The association between *FOXG1* gene and the congenital variant of RTT is relatively recent (6). At present, *FOXG1* point mutations have been reported in 11 congenital RTT patients (6-10). In a recent paper, Kortum and colleagues reported 7 additional patients with a phenotype overlapping both classic and congenital RTT and designed as the *FOXG1* syndrome (11).

FOXG1 is an autosomal gene, located in 14q12. Beside the congenital RTT, due to *FOXG1* point mutations, a 14q12 microdeletion syndrome has been described, in which *FOXG1* is always deleted, together with a variable number of other genes (12, 13). In addition to the severe neurological phenotype, these patients show peculiar facial features including downslanting palpebral fissures, bilateral epicantal folds, depressed nasal bridge, bulbous nasal tip, tented upper lip, everted lower lip and large ears (14, 15). More recently, 14q12 microduplications have been described associated with developmental epilepsy, intellectual disability, and severe speech impairment (16; 17).

FOXG1 gene encodes a DNA-binding transcription factor composed by 489 aminoacids and organized in three main functional domains: the DNA-binding forkhead domain, the GROUCHO-binding domain and the JARID1B binding domain. The interaction of FoxG1 with GROUCHO and JARID1B is required for early brain development. Groucho protein is co-expressed with FoxG1 in telencephalic neuronal progenitor cells and participates in the transcriptional function of FoxG1 by acting as both a co-repressor and an adapter (18). JARID1B is a demethylase capable of removing three methyl groups from histone H3 lysine 4. It plays an important role in regulating chromatin dynamics and can directly regulate gene transcription either alone or as part of a complex with FoxG1 (19). FoxG1 is essential for the

development of the ventral telencephalon in embryonic mammalian forebrain (20). Despite its early expression in telencephalon development, Ariani *et al.* demonstrated that FoxG1 is detectable in the differentiating cortical compartment in the postnatal stages, although at lower levels respect to the early embryonic phases (6). At the single cell level, FoxG1 is localized to the nucleus, outside the heterochromatic foci, suggesting that it is not stably associated with heterochromatin (6). Recently, a report by Le Guen and collaborators demonstrated that a *FOXG1* mutation resulted in mis-localization of FoxG1 to nuclear speckles suggesting that alteration of protein localization inside the nucleus might contribute to its pathological effect (10).

Given the important involvement of MeCP2 in chromatin modifications, RTT has been considered an epigenetic disorder. Indeed, we and others recently provided evidence indicating that different pathological mutations in *MECP2* regulate its chromatin-binding dynamics *in vivo* (21; 22). The epigenetic nature of RTT is further supported by the identification of patients with *FOXG1* mutations. *FOXG1* is in fact involved in global chromatin organization and it plays a key role in regulating neuronal differentiation (23, 24). However, the relationship between FoxG1 and chromatin and its functional role in the nucleus have not been elucidated (19). To address this issue we employed photobleaching strategies, a well accepted assay to study the *in vivo* properties of chromatin binding proteins. Our results suggest that alterations in FoxG1 binding to chromatin and its binding dynamics might contribute to the pathological effects of its mutations and it may explain milder phenotype of the two patients described here.

Material and Methods

Molecular analysis

Blood samples were obtained from patients and their parents after informed consent. DNA was extracted using a QIAmp DNA Blood Kit (Qiagen, Hilden, Germany). The entire *FOXG1* coding sequence (RefSeq NM_005249) was screened as previously described (5, 6).

Cell culture and transfection.

NIH3T3 cells were cultured according to ATCC indications. Cells were plated at 60-70% confluence in a glass chamber for the Leica confocal microscope and transfected using Lipofectamine2000 (Invitrogen) according to the manufacture's instructions. Any further

experimental manipulation was performed 24 hours after transfection. All experiments were performed at 37°C.

Plasmid construction.

To construct the pGFP-*Foxg1* wt vector, the entire cDNA of mouse *Foxg1* was amplified by PCR and the XhoI/BamHI digested product was inserted into pEGFP-C1 (Clontech). The vector containing *Foxg1* cDNA was provided by Dr. Vania Broccoli (Stem Cells and Neurogenesis Unit, Division of Neuroscience, San Raffaele Scientific Institute, Milano, Italy). The constructs for the pathological FOXG1 derivatives were obtained following standard procedures (see supplementary materials). The vector containing the DsRED-MeCP2 was generated inserting MeCP2 cDNA in the DsRED-C1 vector (Clontech); see Marchi et al. 2007 for details (21). The vector carrying the missense mutation p.R244C was kindly provided by Prof. Thierry Bienvenu (10).

Immunofluorescence Microscopy.

Mouse fibroblasts and NIH3T3 were seeded on gelatin-coated glass coverslips and transiently transfected with the above described plasmids using Lipofectamine 2000 (Invitrogen). Twenty hours post-transfection the cells were fixed with 4% paraformaldehyde, permeabilised with 0,05% Triton X-100, and, after blocking with 1% Fetal Bovine Serum, incubated with a polyclonal anti-Foxg1 antibody (ab CAM ab18259). Excess antibody was eliminated and the cells incubated with an anti-rabbit antibody (Alexa 555; Invitrogen). Hoechst 33258 was used to visualise the nuclear compartment. The coverslips were mounted and analysed with an Olympus BX51 Fluorescence microscope. In order to minimize the signal bleed-through between the two acquisition channels in cotransfected cells (red and green) we set the following acquisition parameters for the two channels: pin hole aperture 300, PMT voltage 600 V, PMT offset 1%, objective 40× oil NA 1.25, image size 512×512, frequency scan 400 Hz; green Ch: excitation line 488 nm, laser intensity 2 %, PMT window e00-580 nm and red Ch: excitation line 543 nm, laser intensity 15 %, PMT window 580-670 nm. Cross talk analyses were performed.

Strip-FRAP

Cells eligible for imaging were carefully selected through an imaging-based method where imaging platforms were calibrated by using artificial cells containing EGFP in saline solution (25). Only cells in a range of GFP-FOXG1 concentration between 100-1000 nM were selected for the analysis. Average fluorescence background was evaluated on not-transfected cells and was subtracted from all measurements.

Strip FRAP was performed on a Leica TCS NT confocal microscope with an oil immersion lens (Leica HCX PL APO 40×, NA 1.25-0.75). GFP fluorescence was excited at 488nm with an Ar/K laser and quantified on the Leica platform. Average fluorescence background was evaluated on non-transfected cells and was subtracted from all measurements. The presence of fluorescence artifacts was not masked in any of the images accompanying the paper. The laser power employed during imaging was about 30μW. Data plotting and statistical testing (one or two ways t-test as appropriate) have been performed with the Origin 7.5 package.

Photobleaching was preceded by the acquisition of 64 lines necessary for data normalization. The total fluorescence bleached in the imaging run was estimated by comparing a pre-bleach image of the whole cell with an image acquired at the end of the line scans. Bleaching was performed by scanning the line, chosen to intersect the nucleus, at high power (about 50 times larger than during pre-bleach and recovery) for 160ms. Line scan was performed at a frequency of 400Hz and the recovery was evaluated for 30s. Fluorescence was corrected for background and normalized for the corresponding pre-bleached regions. Recovery curves were fitted by a double exponential function. The immobile fraction was computed by the asymptotic value of the recovery corrected for the total amount of fluorescence loss, as estimated by the comparison of the pre-bleach and post-bleach images.

Results

Clinical description

Patient 1 was a 12.5 year old female. She was born at the 38th week of gestation after an uneventful pregnancy. Auxological parameters and Apgar score were in the normal range. She was a peaceful infant in the first months of life. Deceleration of head growth and developmental delay were apparent from the age of 4 months. She was able to sit at 9 months and to walk independently at 2.5 years. Febrile convulsions appeared at 5 months followed (at

7 months) by atonic afebrile convulsions not completely controlled by therapy. Hand-mouthing stereotypies were reported in the first year of life. At 6 years of age, a bilateral strabismus was surgically corrected. Brain MRI performed at 10 years of age was normal. At the time of our first examination, at 7.5 years, she showed an ataxic gait and no language. She presented postnatal microcephaly (48 cm), midface hypoplasia, slight upslanting palpebral fissures, bulbous nasal tip and anteverted nares, prognathism, diastasis of teeth, thick and everted lower lip and straight hair. At 9.5 years a delayed skeletal maturation was noticed (7.3 years). At the last examination she was 12.5 years, language was absent, she was still able to walk unsupported with a broad base and flexed upper and lower limbs and she still presented atonic seizures. She showed rocking of the trunk, hyperactive behavior and hand apraxia. She had stereotypies of the tongue, protruding out of her mouth, and hand stereotypies: continuously grasping paper and tearing it into little pieces. Hyperventilation was apparent and sleep disturbances and constipation were reported. She showed microcephaly (49.8 cm) with normal height and weight. All specific facial features present at the first examination were more pronounced resulting in a coarse facial appearance (Fig. 1A and 1C).

Karyotype, methylation analysis of the 15q11.2 region, and molecular analysis of *UBE3A, MECP2* and *CDKL5* were normal. Following a clinical suspicion of Kleefstra syndrome array-CGH analysis (Agilent 44K) and *EHMT1* molecular analysis were performed with normal results.

Patient 2 was a 31 year old woman with severe intellectual disability. She was born at term by cesarean section because of abruptio placenta. At birth she showed normal auxological parameters. Right hip dysplasia was diagnosed later. Developmental delay was noticed at four weeks of age because she did not have normal eye contact and she was hypotonic. She was able to sit at 3 years, and to stand with support at 5 years. At the time of our observation she could walk only with support. She wore a corset for scoliosis. As a child, the patient had some slight hand washing stereotypies and sleep disturbances. She has never had seizures. Cerebral CT performed in the first year of life was normal. At the examination she knew about 30 words pronounced unclearly and not always used appropriately. She was also able to use some hand-signs. Her growth parameters were in the normal range with OFC of 54cm (10°-25° percentile). She had coarse facial features with midface hypoplasia, slight upslanting palpebral fissures, bulbous nose and broad nasal bridge, thick lower lip, prognathism, dark, thick and straight hair (Fig. 1B and 1D). Karyotype, array-CGH (Agilent 105K), *MECP2* and *UBE3A* molecular analysis were all normal.

Molecular analysis

FOXG1 molecular analysis revealed one *de novo* mutation in both patients (Fig 2): c.136C>T (p.Gln46X) in patient 1 and c.1200C>A (p.Tyr400X) in patient 2.

GFP-FoxG1 fluorescently tagged mutants and subcellular localization

To examine the effects caused by pathological mutations on FoxG1 subcellular localization, a series of constructs encoding GFP fusion proteins of wild type and mutant FoxG1 were generated (see figure 3).

In order to verify if the cellular localization of the wild type construct corresponded to that described in literature (6; 26), the NIH3T3 cell line was co-transfected with GFP-Foxg1 and DsRED-MeCP2, that binds specifically to heterochromatin (21; 22). Hoechst 33258 was used to visualise the nuclear compartment. As recently indicated in the report of Le Guen et al., the cellular localization of GFP-FoxG1 is mainly nuclear (Figure 3) (10). The comparison between GFP-Foxg1 and DsRED-MeCP2 showed that in the nucleus GFP-Foxg1 was mostly present in euchromatin and it was partially excluded from heterochromatin (Fig 3). To examine the effects caused by pathological mutations on FoxG1 cellular localization, mutants corresponding to the two mutations reported here and to a previously described mutation associated with RTT congenital variant were studied (Fig 4A) (6). After transfection with the Tyr400X and Ser323fsX325 mutants cells with a predominant amount of FoxG1 in the nuclear compartment could be clearly identified (Fig 4B). On the other hand, the N-terminal mutation Gln46X resulted in a clear mislocalization and the fluorescence distribution was both nuclear and cytoplasmatic (Fig 4B).

In order to compare in a quantitative manner the localization in the chromocenters of the FoxG1 wild type with those of the pathological derivatives the chromocenter/nucleoplasmic (Chr/Nuc) ratios of fluorescence intensity was calculated. This ratios was determined by dividing the intensity of the GFP-FoxG1 fluorescence in the chromocenter by that in the nucleoplasmic coronal section around the chromocenter. Data were plotted in Fig 3 panel C. These data demonstrate that the mutants under analysis have lost in a different degree the proper chromatin localization which is typical of FoxG1 WT and therefore they are more dispersed within chromatin: wt GFP-FoxG1 (Chr/Nuc ratio 0.45+/- 0.021), GFP-Q46X (Chr/Nuc ratio 0.75+/- 0.012); GFP-Y400X (Chr/Nuc ratio 0.6+/- 0.029) and GFP-S323fs325X (Chr/Nuc ratio 0.52+/- 0.023) (Fig. 3).

Foxg1 is dynamically bound to chromatin

In order to study the stability of FoxG1 binding to chromatin a photobleaching strategy (strip-FRAP) was adopted. In the FRAP experiments, a powerful light beam is used to irreversibly photobleach the fluorescent molecules in a micron-sized area of the sample (Fig 5A). After photobleaching, bleached molecules will gradually move out of the photobleached area and will be replaced by unbleached molecules. Due to this exchange, the fluorescence inside the photobleached area recovers, and this process is monitored as a function of time (Fig. 5B and C). Since the recovery curves could not be described by a single exponential, to describe the kinetic of the recovery, t_2 (expressed in seconds), which is the time necessary for the fluorescence to reach half of the total recovery was used. As shown in Figure 5D, fluorescence recovery and chromatin affinity decrease with the extension of the protein deletion (t_2 of GFP-FoxG1 wild type=3,08 +/- 0,31 Vs 0,9 +/- 0,09 in GFP-FoxG1 Y400X, 0,67 +/- 0,02 in GFP-FoxG1 S323fsX325 and 0,47 +/- 0,01 in GFP-FoxG1 Q46X) demonstrating that different parts of the protein participate to chromatin binding. On the other hand, the immobile fraction did not decrease gradually with the extension of protein deletion but it was significantly lower for Tyr400X and Gln46X constructs while in the case of Ser323fsX325 it was not statistically different from the WT (Fig 5D and tables 1 and 2). Interestingly, the single pathological missense mutation p.R244C (present in the FHD) significantly impaired the capability of GFP-FoxG1 to bind chromatin (t_2 WT 3.08+/-0.31s vs t_2 p.R244C 1.86+/-0.25s), as well as diminished the immobile fraction (IF WT 0.17+/-0,02 vs IF p.R244C 0.06+/-0.03).

Discussion

Since the first description in 2008, a total of 19 patients with *FOXG1* pathogenic point mutations have been reported: 11 congenital RTT patients, 1 classic RTT patient and 7 patients with an homogeneous phenotype designated as the *FOXG1* syndrome and characterized by postnatal microcephaly, severe intellectual disability, dyskinesia and brain abnormalities (5-11). We report here two unrelated patients with a de novo *FOXG1* point mutation, p.Gln46X and p.Tyr400X, respectively. These patients have RTT features including normal prenatal and perinatal period, hand apraxia, previous hand stereotypies (hand-mouthing and hand-washing type) and impaired sleep patterns. Postnatal microcephaly, hyperventilation and constipation were present in Patient 1 and severe scoliosis was present in

patient 2. Both patients were able to walk, the younger unsupported and the older with support. The two patients showed many characteristics typical of RTT. However, according to the revised diagnostic criteria for RTT, their phenotype did not fit with either classic or variants of RTT (1). Furthermore, their clinical characteristics were undoubtedly milder than the phenotype previously associated with *FOXG1* mutations. While all previously reported patients showed postnatal microcephaly, one of the patients presented here, Patient 2, had normal OFC. Both patients had quite good motor abilities and were able to walk. It is worth noting that only 3/19 patients previously reported with *FOXG1* mutations were able to walk and one of them had the same late truncating mutation of Patient 2 of this study (p.Y400X) (5, 10, 11). Therefore, we hypothesize that specific *FOXG1* mutations may correlate with a milder phenotype.

In order to clarify the pathogenic mechanisms of *FOXG1*-associated disease, we investigated the relationship between FoxG1 and chromatin. Since the crucial event for FoxG1 action is its binding to chromatin, it is essential to know if this binding is static or dynamic, and whether pathogenic mutations modify the binding and/or the distribution of the protein among cell compartments. Strip-FRAP experiments showed that GFP-FoxG1 WT binding to chromatin is reversible, but a significant fraction of the total protein, during the time of observation, was stably bound. Thus, it is tempting to speculate that these two binding states reflect two different roles of FoxG1: the reversibly bound fraction might be associated with the modulation of gene expression, while stably bound FoxG1 might operate as a structural protein involved in chromatin organization and long term gene repression.

We subsequently tested and compared the distribution, binding and mobility of three FoxG1 derivatives, the two mutations reported here and a previously reported mutation associated with congenital variant (6). Our experiments showed that even a small deletion of FoxG1, like that seen in p.Tyr400X, caused a dramatic reduction in chromatin affinity. Chromatin binding further decreased with the extension of deletion. However, this progressive reduction of affinity did not seem to be related to the severity of symptoms in RTT patients, since the p.Gln46X mutation, that totally impairs binding to chromatin, causes a milder RTT phenotype. Interestingly, the value of the immobile fraction is not related to the decrease in chromatin affinity and with the extension of protein deletion. Moreover, the immobile fraction appeared significantly higher for the mutation p.Ser323fsX325, that is associated with the most severe RTT phenotype (6). These data clearly indicate that (i) protein integrity is crucial to determine chromatin binding; (ii) several regions of the protein contribute to chromatin binding; (iii) the change in chromatin affinity is not a relevant read-

out for the severity of RTT symptoms; and (iv) the immobile fraction could be a relevant read-out for the severity of RTT symptoms.

To reconcile these findings with the patho-physiological scenario it is worth recalling that RTT patients carrying *FOXG1* mutations are heterozygotes and in the same cell both the mutated and wt proteins coexist, each with its specific chromatin interaction dynamics. It is tempting to speculate that the severity of symptoms, at least for the conditions examined here, could be attributed to that fraction of the protein which is not able to be exchanged as a consequence of the mutation and thus remains stably bound to chromatin (immobile fraction). Thus, these changes in immobile fraction observed in p.Ser323fsX325 could be caused by the formation of large complexes or protein dimers. If the dimers or complexes are stably bound to the chromatin, only the movement of the monomers, providing a certain t_2, will be detected whereas the stuck percentage will be measured as immobile fraction.

The Ser323fsX325 mutation, presenting a significantly higher immobile fraction as compared to Gln46X and Tyr400X, could act by excluding the access to chromatin of the wt FoxG1 protein, thus preventing its normal action. In this way, the high fraction of FoxG1 irreversibly bound to chromatin in specific pathological derivatives, such as Ser323fsX325, could decrease or even prevent the action of the barely sufficient wt FoxG1 protein produced by the second allele. Conversely, the Gln46X mutation that almost abolishes the protein, might not impair the activity of wt FoxG1 protein and thus result in a milder RTT phenotype. Nevertheless, it is worth noting that two reported patients with the earliest truncating mutations (p.R86X and p.R88PfsX99) had a phenotype characterized by severe postnatal microcephaly and severe motor and cognitive impairment (they did not learn the ability to sit) (11). This phenotypic difference may imply the presence of a functional domain between amino acids 46 and 86, not yet identified.

Usually, patients with *FOXG1* mutations do not show peculiar facial features in contrast with patients with 14q12 microdeletion syndrome. Unexpectedly, the two patients presented here have peculiar and strikingly similar facial features (Fig. 1), although different from that reported in the 14q12 microdeletion syndrome (14). The facial gestalt of both patients is evocative of the Kleefstra syndrome (OMIM#607001) normally due to *EHMT1* mutations; both patients had a flat face with anteverted nares, thickened lower lip and slightly upslanting palpebral fissures. Although everted lower lip, bulbous nasal tip and tongue protrusion are present in both Kleefstra and 14q12 microdeletion syndrome, the facial gestalt of these two patients was more consistent with the *EHMT1*-associated phenotypic spectrum. Interestingly, both FoxG1 and EHMT1 proteins interact with members of JARID1 family and are involved

in modulation of the chromatin structure. In this perspective, the overlapping phenotype described in this paper could not be completely unexpected. Further experiments are necessary in order to clarify the relationship between *FOXG1* and *EHMT1*.

Acknowledgements

References

1. Neul JL, Kaufmann WE, Glaze DG, Christodoulou J, Clarke AJ, Bahi-Buisson N *et al.* Rett syndrome: revised diagnostic criteria and nomenclature. Ann Neurol 2011: 68 (6): 944-950.

2. Huppke P, Laccone F, Kramer N, Engel W and Hanefeld F. Rett syndrome: analysis of *MECP2* and clinical characterization of 31 patients. Hum Mol Genet. 2000: 9 1369-1375.

3. Monros E, Armstrong J, Aibar E, Poo P, Canos I and Pineda M. Rett syndrome in Spain: mutation analysis and clinical correlations. Brain Dev 2001: Suppl 1 S251-253.

4. Smeets E, Schollen E, Moog U, Matthijs G, Herbergs J, Smeets H *et al.* Rett syndrome in adolescent and adult females: clinical and molecular genetic findings. Am J Med Genet A 2003: 122 (3): 227-233.

5. Philippe C, Amsallem D, Francannet C, Lambert L, Saunier A, Verneau F *et al.* Phenotypic variability in Rett syndrome associated with FOXG1 mutations in females. J Med Genet 2010: 47 (1): 59-65.

6. Ariani F, Hayek G, Rondinella D, Artuso R, Mencarelli MA, Spanhol-Rosseto A *et al.* FOXG1 is responsible for the congenital variant of Rett syndrome. Am J Hum Genet 2008: 83 (1): 89-93.

7. Bahi-Buisson N, Nectoux J, Girard B, Van Esch H, De Ravel T, Boddaert N *et al.* Revisiting the phenotype associated with FOXG1 mutations: two novel cases of congenital Rett variant. Neurogenetics 2010: 11 (2): 241-249.

8. Mencarelli MA, Spanhol-Rosseto A, Artuso R, Rondinella D, De Filippis R, Bahi-Buisson N *et al.* Novel FOXG1 mutations associated with the congenital variant of Rett syndrome. J Med Genet 2010: 47 (1): 49-53.

9. Le Guen T, Bahi-Buisson N, Nectoux J, Boddaert N, Fichou Y, Diebold B *et al.* A FOXG1 mutation in a boy with congenital variant of Rett syndrome. Neurogenetics 2011: 12 (1): 1-8.

10. Le Guen T, Fichou Y, Nectoux J, Bahi-Buisson N, Rivier F, Boddaert N *et al.* A missense mutation within the fork-head domain of the forkhead box G1 Gene (FOXG1) affects its nuclear localization. Hum Mutat 2011: 32 (2): E2026-2035.

11. Kortum F, Das S, Flindt M, Morris-Rosendahl DJ, Stefanova I, Goldstein A *et al.* The core FOXG1 syndrome phenotype consists of postnatal microcephaly, severe mental retardation, absent language, dyskinesia, and corpus callosum hypogenesis. J Med Genet 2011: 48 (6): 396-406.

12. Bisgaard AM, Kirchhoff M, Tumer Z, Jepsen B, Brondum-Nielsen K, Cohen M *et al.* Additional chromosomal abnormalities in patients with a previously detected abnormal karyotype, mental retardation, and dysmorphic features. Am J Med Genet A 2006: 140 (20): 2180-2187.

13. Papa FT, Mencarelli Ma, Caselli R, Katzaki E, Sampieri K, Meloni I *et al.* A 3 Mb deletion in 14q12 causes severe mental retardation, mild facial dysmorphisms and Rett-like features. Am J Med Genet A 2008: 146A (15): 1994-1998.

14. Mencarelli MA, Kleefstra T, Katzaki E, Papa FT, Cohen M, Pfundt R *et al.* 14q12 Microdeletion syndrome and congenital variant of Rett syndrome. Eur J Med Genet 2009: 52 (2-3): 148-152.

15. Jacob FD, Ramaswamy V, Andersen J and Bolduc FV. Atypical Rett syndrome with selective FOXG1 deletion detected by comparative genomic hybridization: case report and review of literature. Eur J Hum Genet 2009: 17 (12): 1577-1581.

16. Brunetti-Pierri N, Paciorkowski AR, Ciccone R, Mina ED, Bonaglia MC, Borgatti R, *et al*. Duplications of FOXG1 in 14q12 are associated with developmental epilepsy,

mental retardation, and severe speech impairment. Eur J Hum Genet 2011: 19 (1):102-7.

17. Yeung A, Bruno D, Scheffer IE, Carranza D, Burgess T, Slater HR *et al*. 4.45 Mb microduplication in chromosome band 14q12 including FOXG1 in a girl with refractory epilepsy and intellectual impairment. Eur J Med Genet 2009: 52 (6): 440-442.

18. Yao J, Lai E and Stifani S. The winged-helix protein brain factor 1 interacts with groucho and hes proteins to repress transcription. Mol Cell Biol 2001: 21 (6): 1962-1972.

19. Roesch A, Mueller AM, Stempfl T, Moehle C, Landthaler M and Vogt T. RBP2-H1/JARID1B is a transcriptional regulator with a tumor suppressive potential in melanoma cells. Int J Cancer 2008: 122 (5): 1047-1057.

20. Martynoga B, Morrison H, Price DJ and Mason JO. Foxg1 is required for specification of ventral telencephalon and region-specific regulation of dorsal telencephalic precursor proliferation and apoptosis. Dev Biol 2005: 283 (1): 113-127.

21. Marchi M, Guarda A, Bergo A, Landsberger N, Kilstrup-Nielsen C, Ratto Gm *et al.* Spatio-temporal dynamics and localization of MeCP2 and pathological mutants in living cells. Epigenetics 2007: 2 (3): 187-197.

22. Kumar A, Kamboj S, Malone BM, Kudo S, Twiss JL, Czymmek KJ *et al.* Analysis of protein domains and Rett syndrome mutations indicate that multiple regions influence chromatin-binding dynamics of the chromatin-associated protein MECP2 in vivo. J Cell Sci 2008: 121 (Pt 7): 1128-1137.

23. Brancaccio M, Pivetta C, Granzotto M, Filippis C and Mallamaci A. Emx2 and Foxg1 inhibit gliogenesis and promote neuronogenesis. Stem Cells 2010: 28 (7): 1206-1218.

24. Dastidar SG, Landrieu PM and D'mello SR. FoxG1 promotes the survival of postmitotic neurons. J Neurosci 2011: 31 (2): 402-413.

25. Costa M, Marchi M, Cardarelli F, Roy A, Beltram F, Maffei L , Ratto GM. Dynamic regulation of ERK2 nuclear translocation and mobility in living cells. J Cell Sci 2006: 119 (Pt 23): 4952-63.

26. Regad T, Roth M, Bredenkamp N, Illing N and Papalopulu N. The neural progenitor-specifying activity of FoxG1 is antagonistically regulated by CKI and FGF. Nat Cell Biol 2007: 9 (5): 531-540.

Tables and Figures

Table 1
t-test p values of immobile fraction

immobile fraction	*FOXG1* WT	*FOXG1* R244C	*FOXG1* Y400X	*FOXG1* S323fsX325	*FOXG1* Q46X	GFP
FOXG1 WT						
FOXG1 R244C	0.001					
FOXG1 Y400X	0.031	N.S.				
FOXG1 S323fsX325	N.S.	0.018	$<10^{-4}$			
FOXG1 Q46X	$<10^{-5}$	N.S.	N.S.	$<10^{-6}$		
GFP	$<10^{-5}$	0.045	$<10^{-4}$	$<10^{-10}$	$<10^{-3}$	

Table 2
t-test p values of T_2

T_2	*FOXG1* WT	*FOXG1* R244C	*FOXG1* Y400X	*FOXG1* S323fsX325	*FOXG1* Q46X	GFP
FOXG1 WT						
FOXG1 R244C	0.007					
FOXG1 Y400X	0.002	0,042				
FOXG1 S323fsX325	$<10^{-5}$	$<10^{-3}$	N.S.			
FOXG1 Q46X	$<10^{-8}$	$<10^{-3}$	$<10^{-6}$	$<10^{-4}$		
GFP	$<10^{-4}$	$<10^{-3}$	$<10^{-4}$	0.002	N.S.	

The table reports the p values of the t-test between all the measured T2 of the different proteins investigated. N.S.: Not Significative ($p>0.05$)
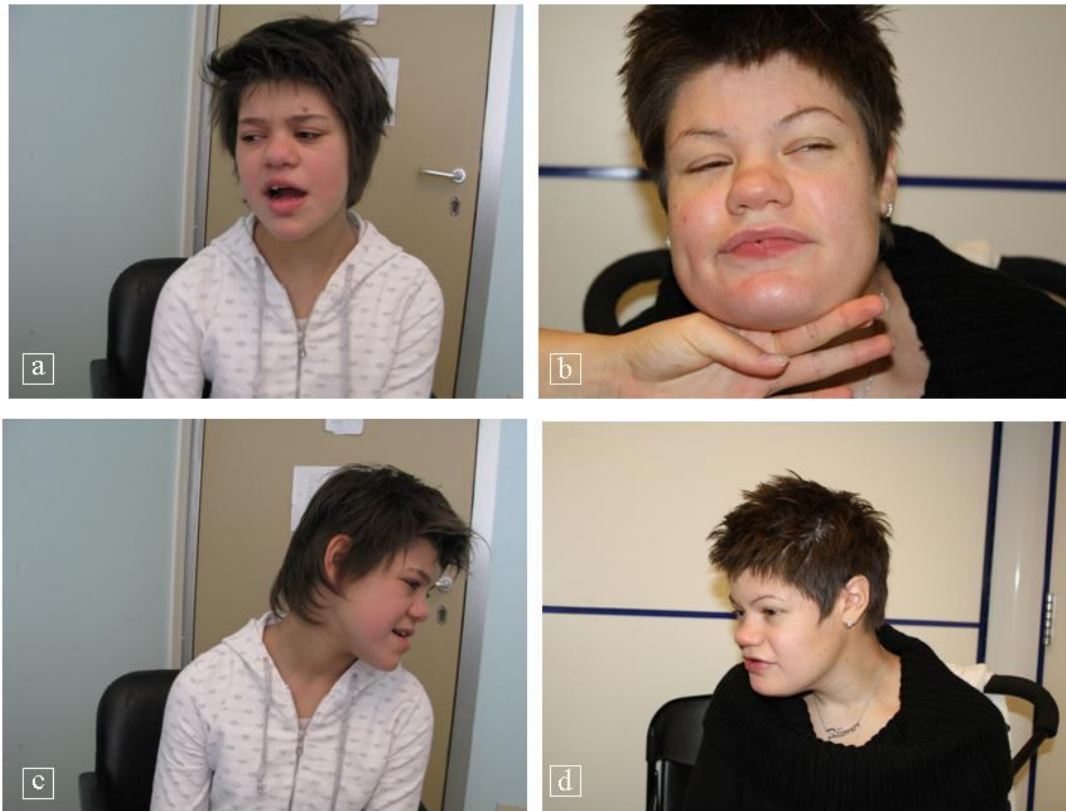
Figure 1. Pictures of the two patients front (A) and lateral (C) view of patient 1. Front (B) and lateral (D) view of patient 2.
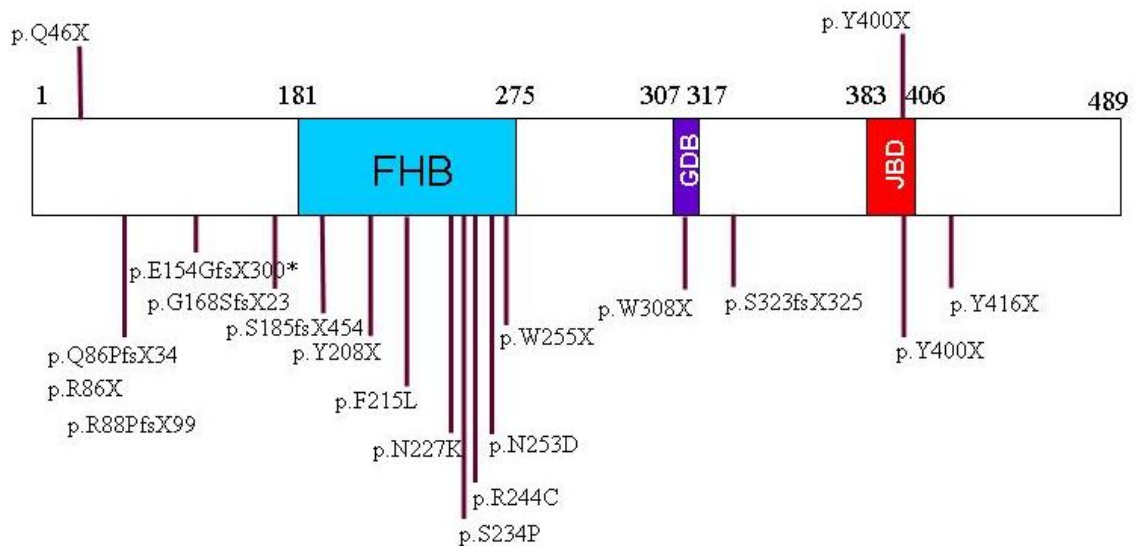
Fig. 2 *FOXG1* mutations. Schematic representation of the protein with its functional domains. Mutations already reported in the literature are indicated on the bottom; * identifies a mutation reported in three patients. The two mutations reported in the present article are shown on the top.
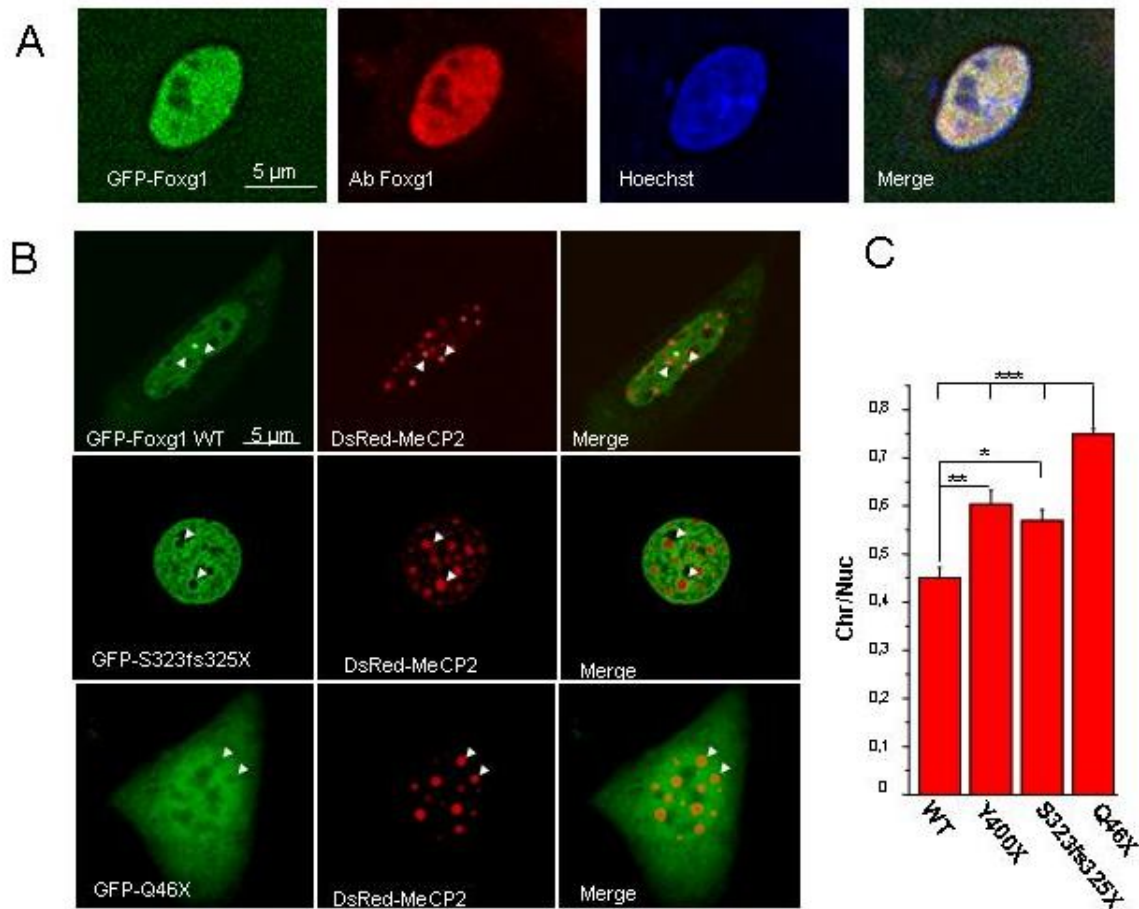
Fig.3 Co-expression and distribution of DsRed-MeCP2 and GFP-Foxg1 protein in NIH3T3 cells. A) Co-localization of Hoechst and GFP-Foxg1 in NIH3T3 (bar 5 µm) in GFP-Foxg1 transfected NIH3T3 cells. In green GFP-FoxG1 fluorescence. In red immunofluorescence against Foxg1. In blue Hoechst staining. In the last picture the merge of the three channels shows that Foxg1 co-localizes with the hoechst staining and the fluorescent fusion protein has a similar distribution. B) Co-expression and distribution of DsRed-MeCP2 and GFP-FoxG1 WT, GFP-S323fs325X, GFP-Q46X protein in NIH3T3 cell line. On the left: distribution of GFP-FoxG1, GFP-S323fs325X, and GFP-Q46X (Green channel), in the middle distribution of DsRed-MeCP2 (red channel) shows the typical heterochromatic localization of MeCP2 (chromocenters). In the right: merge of the two channels. Arrows indicate the position of two chromocenters. C) Comparison of Chr/Nuc ratio of FoxG1 wild type with the pathological derivatives: GFP-Y400X, GFP-S323fs325X and GFP-Q46X . *** p≤0.001; ** p≤0.01; * p≤0.05.
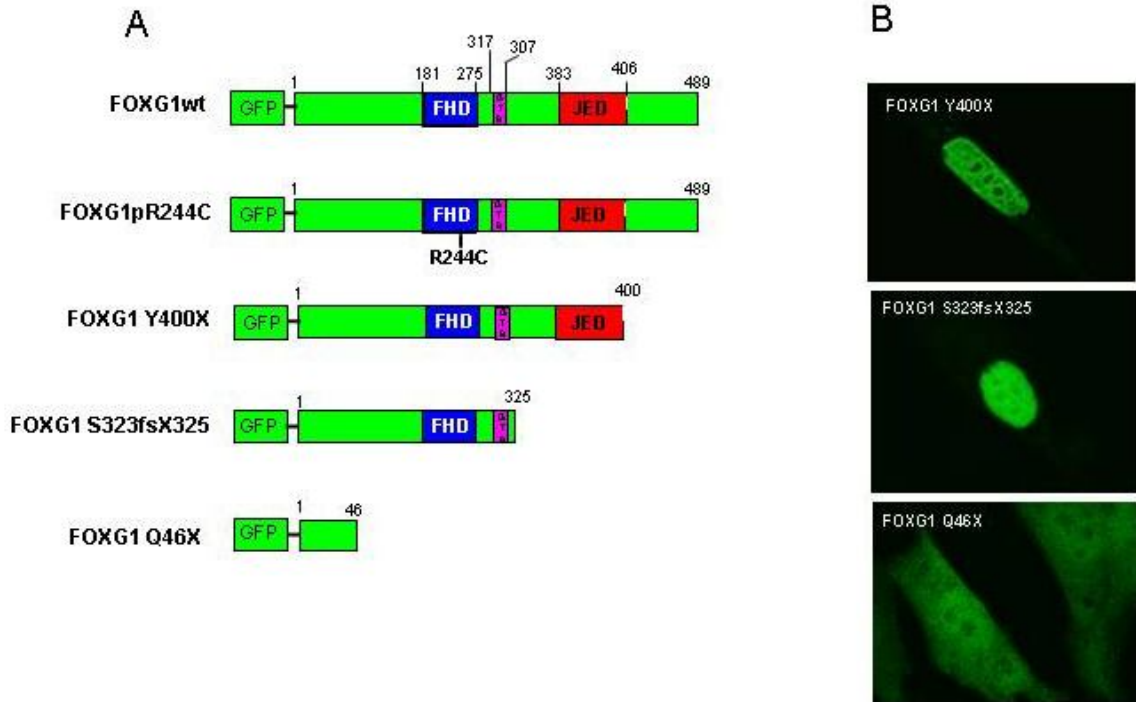
Fig. 4 GFP-FoxG1 fluorescently tagged mutants and their subcellular localization.
A) Schematic representation of the constructs used in this study with the definition of the functional regions and the location of nonsense mutations. WT: Wild Type, FHD: Fork Head Domain; GTB: GROUCHO/TLE-Binding domain; JED: JARID1B Binding Domain. B) Representative images of transfected cells showing the intracellular localization of the different constructs. GFP-Y400X, GFP-Ser323fsX325 and GFP-R244C (data not shown) retain nuclear localization while GFP-Q46X construct is diffusely distributed in both nucleus and cytoplasm.
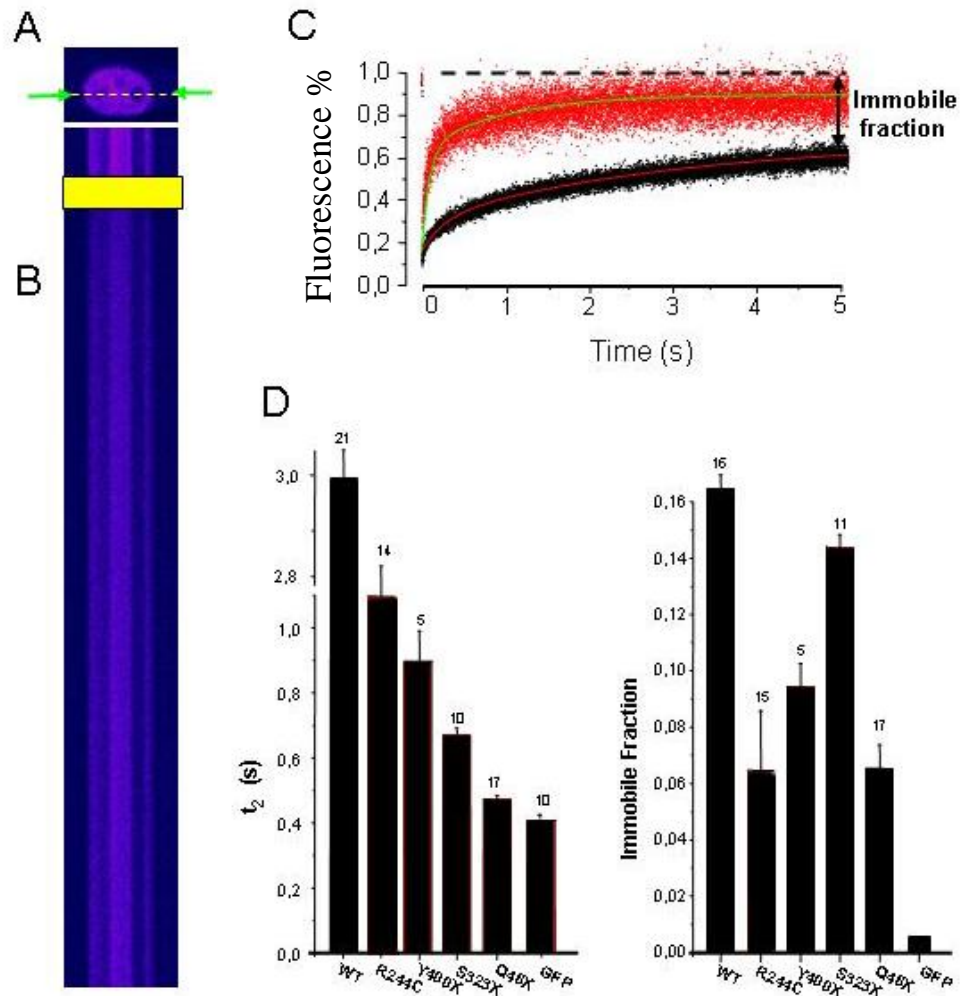
Fig. 5. Relative mobility of FoxG1 in the nuclear compartment. A) High resolution imaging of a NIH3T3 transfected with GFP-FoxG1. To assess the mobility of the protein at an high time resolution, repetitive line scans were performed along the line indicated by the green arrows. Pseudo color were used to improve the readability of the image. Calibration bar 10 μm. B) Time series showing the fluorescence intensity across the scanned line. The photobleaching, indicated by the yellow rectangle, is followed by the gradual recovery of fluorescence. C) Quantification of the signal intensity in the nucleus of WT and p.Q46X (black and red line, respectively). In this case the t_2 were 3.02 s and 0.47 s (WT and p.Q46X respectively) and the immobile fractions were 0.17 and 0.07. D) Summary of average values for t_2 and immobile fraction measured in cells transfected with GFP-FoxG1 wt, GFP-R242C, GFP-Tyr400X, GFP-Ser323fsX325, GFP-Gln46X and GFP alone. Numbers indicate the sample size and bars are standard errors. The p values are in the tables in the supplementary materials.

5. RESULTS-3

5.1 Introduction

Rett Syndrome (RTT) is a neurological disorder that affects principally females (incidence 1:10.000 live female birth) representing the most common cause of mental retardation in girls. Clinical signs manifest in patients during childhood, after an apparently normal developmental period (6-18 months of life); however not all the symptoms are prominent initially, but rather appear over stages. RTT is an heterogeneous diseases both from clinical and from genetic point of view; in fact, beside the classic form, several variants have been described and mutations in three different genes have been associated to this syndrome: *MECP2* and *CDKL5*, located on X-chromosome, and *FOXG1* located on chromosome 14. About 80% of RTT cases are caused by mutations in *MECP2* and both mouse and human cellular models have been developed to investigate the main molecular mechanisms that lead to RTT Syndrome. In 2007 the technology of genetic reprogramming allowed to generate induced pluripotent stem cells (iPSCs) representing an unprecedented tool to create good *in vitro* human cellular models. iPSCs can be generated from somatic cells, such as adult dermal fibroblasts, through the retroviral transduction of a set of transcription factors related to pluripotency, namely OCT-4, SOX-2, c-MYC and KLF-4 (Yamanaka's factors). The iPSCs obtained are very similar to embryonic stem cells (ESCs) as regards their morphology, proliferation, gene expression, *in vitro* differentiation and teratoma formation. Moreover, like ESCs, they can be expanded indefinitely *in vitro* and can be differentiated into different cell types. Up to date, iPSCs have been generated from patients with both neurodegenerative (ALS, SMA, Parkinson, HD and FD) and neurodevelopmental (FRAXA, PW-AS) disorders and in some cases neuronal differentiation has been performed using protocols developed for ESCs. Recently, Marchetto et al derived iPSCs from *MECP2*-mutated fibroblasts in order to generate a human model for Rett syndrome. In RTT iPSC-derived glutamatergic neurons they observed a reduction of synapses and dendritic spines compared to controls. In addition, electrophysiological analysis revealed that RTT neurons have a significant decrease in the frequency and in the amplitude of spontaneous synaptic currents respect to wild type neurons. All these results are in accordance with findings in mouse models underlying that iPSCs technology could be useful to model RTT *in vitro*.

To date, the role of FoxG1 during early forebrain development has been investigated in knock-down mice. In particular, these studies revealed that FoxG1 mutant brains show an important reduction of telencephalic vescicles compromising the correct development of the telencephalon. Compatible with these findings, FoxG1 is expressed in the proliferating neuroepitelium other than the developing retina, optic stalks and superior colliculus. In addition, FoxG1 is also implicated in regulating cortical arealization, expansion of the cortical progenitor pool and regulation of progenitor cell-cycle length [47,55,56,59]. In neuroepitelial cells, FoxG1 regulates proliferation through inhibition of FoxO-Smad transcriptional complex and, therefore, it is able to block p21Cip1 induction by TGF-beta signals [49,50].

In spite of all findings about FoxG1 function in progenitor cells proliferation, its role during neuronal differentiation has not been elucidated jet. The principal limitation to this investigation is due to the premature death of *Foxg1* homozygous mutant mice and, for this reason, recent studies have been focused on heterozygous FoxG1$^{+/-}$ mice that can reach adulthood. Morphological and behavioral studies in *Foxg1*$^{+/-}$ mice reveal a severe microcephaly, altered hippocampal neurogenesis and behavioral and cognitive delay respect to controls [60,74,75].

Despite this mouse model recapitulates the principal clinical course of RTT, it cannot faithfully recapitulate the human condition; in addition this model ignore the influence of genetic background on disease phenotype. To solve these issues and establish a human model for *FOXG1*-related disease we decided to set up the protocol for genetic reprogramming in order to obtain iPSCs from fibroblasts of RTT patients carrying *FOXG1* mutations and unaffected controls and then differentiate them into neuronal cells.

5.2 Experimental Procedures

Patients

For the set up of the reprogramming protocol we have selected two patients (25 and 10 years old) with a clinical diagnosis of congenital variant of RTT presenting mutations in *FOXG1* gene (p.W255X and p.S323fsX325 respectively). The clinical course of these patients fulfilled the international criteria for RTT variants. Detailed clinical information is reported in Ariani et al 2008 [31].

Cell cultures

Fibroblasts Female RTT fibroblasts were isolated from skin biopsies (about 3-4 mm^3) performed using the Punch Biopsy procedure following informed consent signature. Fibroblasts at passage 2 or 3 were cultured in high glucose-DMEM (containing 10% (vol/vol) FBS, 50 U ml^{-1} penicillin and 50 mg ml^{-1} streptomycin) with standard protocols and then reprogrammed following the protocol by Hotta et al as detailed below [76].

HEK293T (human embryonic kidney 293T) and **PLAT-E** cell lines were grown at 37°C under humidified air containing 5% CO_2 in VP medium (high glucose-DMEM containing 10% (vol/vol) FBS, 0.1 mM non-essential amino acids, 50 U ml^{-1} penicillin and 50 mg ml^{-1} streptomycin).

Lentivirus production

HEK293T cells were plated at a density of 6×10^6 cells in three T-75 flasks with filter cap (one for each expression vector) and incubated overnight. Cells were transfected with 15 µg of each lentiviral vector plasmid (PL-SIN-PGK-EiP; PL-SIN-EOS-C(3+)-EiP; pLenti6-UbC-mSlc7a1), together with 10 µg of four packaging plasmids encoding the lentiviral *Gag-pol, Tat, Rev* and *VSV-G* proteins by Lipofectamine 2000 reagent (Invitrogen). After 8-16 hours from transfection, the medium was replaced with 25 ml of fresh and pre-warmed (37°) VP medium. Two days after transfection, we harvested media containing the virus into a 50 ml centrifuge tube and we proceeded with concentration. We stored 500 µl of medium at 4°C for evaluation of titer of un-concentrated virus (see below). For virus concentration we used two different kits, following manufacturers protocol: ViraBind (CellBiolabs) and Fast-Trap (Millipore). After concentration, lentiviral vector titration was performed for PL-SIN-PGK-EiP in order to determine how many lentiviral particles are present in 1 ml of preparation (Infectous Unit/ml). One day before titration, we seeded HEK293T cells at a density of 10^5 cells per well of a 12-well plate. The cells were then infected with several ten-fold serial dilutions of both concentrated and un-concentrated lentiviral vector into VP medium containing polybrene at 8 µg/ml. After 8-16 hours of infection, we changed the medium with fresh HEK293T medium in order to remove virus and polybrene. The percentage of infected cells was estimated by immunostaining with an Anti-GFP antibody and the viral titer was then calculated by using the following formula:

$$\text{Viral titer (IU/ml)} = \frac{[\text{Infected cells number in a well}] \times [\text{EGFP+\%/100}]}{[\text{Amount of virus used (ml)}]}$$

Since the three lentivirus are produced in parallel, we assumed that the titer of PL-SIN-PGK-EiP corresponds approximately to that of PL-SIN-EOS-C(3+)-EiP and pLenti6-UbC-mSlc7a1.

Retrovirus preparation

Plat-E packaging cells were used for retrovirus production. Cells were seeded at a density of 2.5×10^6 cells into four T-25 flasks and incubated over-night. The next day, a mix composed by: Opti-MEM I medium, 10 µg of each of Yamanka's factors pMXs-hOCT4, pMXs-hSOX2, pMXs-hKFL4, pMXs-hC-MYC (one plasmid in each tube) and Lipofectamine 2000 was prepared and incubated for 20 minutes at room temperature. During incubation, culture medium was aspirated from cells and 4 ml of pre-warmed fresh VP medium was gently added into the four flasks. Finally, we added drop-wise 1 ml of DNA-Lipofectamine complexes to each flask and kept them at 37°C in a 5% CO_2 incubator overnight. After 8-16 hours from the transfection the old medium was discarded and 5 ml of pre-warmed fresh VP medium was added. Virus-containing medium was harvested 24 hours later and passed through a 0.45 µm syringe filter to remove cell debris. About 4-5 ml of each retroviral vector are obtained and ready for infection into human fibroblasts.

Fibroblast infection with Lentiviral vectors

Human RTT fibroblasts were seeded into two T-25 flasks at 2.5×10^5 cells per flask whit 5 ml of fibroblasts medium one day before infection. The day after, the medium was changed with fresh fibroblast medium containing polybrene at 8 µg/ml and one of the two lentiviral vectors PL-SIN-EOS-C(3+)-EiP and PL-SIN-PGK-EiP (control infection) was added to each flask. The amount of lentiviral vector was determined on the basis of the titer of lentiviral preparation and the desired "multiplicity of infection" (MOI) that can be estimated by using the following formula:

$$\text{MOI} = \frac{[\text{Viral titer (IUml}^{-1})] \times [\text{Amount of virus used for infection (ml)}]}{[\text{Target cell number}]}$$

The MOI indicates how many lentiviral vectors are integrated in a single cell; this value is important for the successful use of lentiviral vectors and it is critical to establish the MOI by proper titration in order to attain an high infection efficiency and restrict multi-copy integrations of the virus. A MOI between 2 and 10 is suggested in the original protocol to achieve high infection efficiency.

Eight to sixteen hours after the infection the medium was changed with fresh fibroblast medium (5ml) containing polybrene at 8 µg/ml. An infection with pLenti6-UbC-mSlc7a1 was performed for the flask infected with PL-SIN-EOS-C(3+)-EiP. The medium was changed to fresh fibroblasts medium 8 to 16 hours after infection. Two days after infection with pLenti6-UbC-mSlc7a1 lentiviral vector, we added the selected amount of Blasticidin into culture medium to select for pLenti6-UbC-mSlc7a1 infected cells. In fact, this vector encodes for Blasticidin resistance allowing the selective survival of infected cells. The same concentration of Blasticidin was added also to PGK-infected flask as a negative control for selection. We continued to change the medium every day with the addition of Blasticidin. Within 4-7 days of selection, almost all the cells in the PGK-infected flask should be killed by Blasticidin. Once all PGK-infected cells were dead, we stopped selection in pLenti6-UbC-mSlc7a1 infected flask and expanded cells by adding fresh medium.

Fibroblast infection with reprogramming retrovirus vectors

Human fibroblasts expressing mouse mSlc7a1 gene were seeded at 1×10^5 cells per well in 2 wells of a 6 well plate. Two infections with the reprogramming retroviral vectors are necessary to obtain a good efficiency. For the infection, 0.5 ml of the pMXs-hOCT4, pMXs-hSOX2, pMXs-hKFL4, and pMXs-hC-MYC retroviral vectors were added to each well together with Polybrene at a final concentration of 8 µg/ml. The day after, virus-containing medium was replaced with fresh fibroblast medium. The medium was changed every 2 days until 7 days after the first infection. At this point, fibroblasts were trypsinized and plated on Matrigel-coated dishes (working concentration 0.166 mg/ml). The day after, the medium was changed to mTeSR1 medium (Stem Cell Technologies) that should be changed every 2 days until iPS colonies become evident (around 2-3 weeks post induction).

Immunostaining

Cells grown on coverslips were fixed in 4% paraformaldehyde (PFA) (prepared in fresh PBS 1×) for 10 minutes at 37 °C, quenched for 20 minutes in 50 mM ammonium

chloride and permeabilized with 1× PBS/0.01% Triton X-100 for 10 minutes. Two hours of incubation with blocking buffer (2% FBS, 2% BSA and 0.2% fish skin gelatin in 1× PBS) were performed. After blocking, coverslips were incubated for 1 hour with the primary antibody anti-GFP (Ab-cam) diluted 1:1000 in 1× PBS–10% blocking solution, and washed 3 times with 1× PBS. Finally, the coverslips were incubated for 30 minutes with the secondary antibody (*Alexa* Fluor 488 goat anti-rabbit IgG) diluted 1:1000 in 1× PBS–10% blocking solution. The coverslips were then washed 3 times with 1× PBS and stained with DAPI 1µg/ml in 1× PBS for 10 minutes. Coverslips were mounted with Mowiol and observed with an Axioscope 40FL (Zeiss) microscope connected to a computer. Images were acquired with the "Isis" program and merged and analyzed using ImageJ.

5.3 Results

In order to reprogram patient's fibroblasts we decided to apply a published protocol (Hotta et al) which consists in the use of mouse-specific retroviral vectors carrying the four Yamanaka's factors (OCT4, SOX2, KFL4 and c-MYC). The retrovirus infection is obtained through the previous infection with a lentivirus that induces the expression of an ecotropic retrovirus receptor (mouse Slc7a1 gene). This method guarantee an higher level of safety for the operator since only target human cells expressing mSlc7a1 receptor can be infected. Moreover, the application of this protocol has another important advantage since it allows to make a step by step selection of reprogrammed cells through the expression of a stem cell-specific cassette. The cassette is named EOS (ETn, Oct-4 and Sox-2) and it is activated upon reprogramming into iPS cells to induce the expression of an enhanced green fluorescence protein (EGFP) and a puromycin resistance gene; in fact these two reporter genes are under the transcriptional control of sequences from the promoters of the pluripotent state-specific transcriptional factors Oct-4 and Sox-2 and the stem-cell specific transposon ETn. The activation of this expression cassette allows to select fully reprogrammed cells.

Following the protocol, we produced lentiviral vectors (EOS, PGK and mSlc7a1) into HEK293T cells. Considering that EOS expression is activated only in iPS cells, it is necessary to simultaneously produce a control vector expressing GFP under the control of the ubiquitous PGK (phosphoglycerate kinase 1) promoter in order to estimate the viral titer in HEK293T cells. Given that the viruses are prepared and concentrated in parallel, the titer of PGK is considered indicative of the titer of the other two lentivirus.

To concentrate the obtained viruses we firstly used the lentiviral concentrator kit ViraBind (CellBiolabs). Viral titer was calculated by infection of HEK293T cells with several

ten-fold serial dilutions of PGK-EGFP virus and the subsequent count of EGFP-positive cells. Titration was performed for both concentrated and un-concentrated virus and the viral titer (IU/ml) was calculated at 48 hours and 5 die from infection. The original protocol asserts that the obtained viral titer should be of 10^5 to 10^6 IU/ml without concentration. Using the ViraBind concentrator kit we expected to obtain an increase in viral titer by 3 fold (100 µl of highly purified lentivirus). However, we obtained a viral titer of $1,02 \times 10^5$ IU/ml for the un-concentrated and $3,9 \times 10^5$ IU/ml for the concentrated virus; thus no significant increase in titer was observed after concentration. A second attempt was performed using the Fast-Trap kit (Millipore) for viral concentration. Using this kit we obtained an increase in viral titer after concentration since the titer was 1.7×10^6 IU/ml, but it was still low (Fig.1).
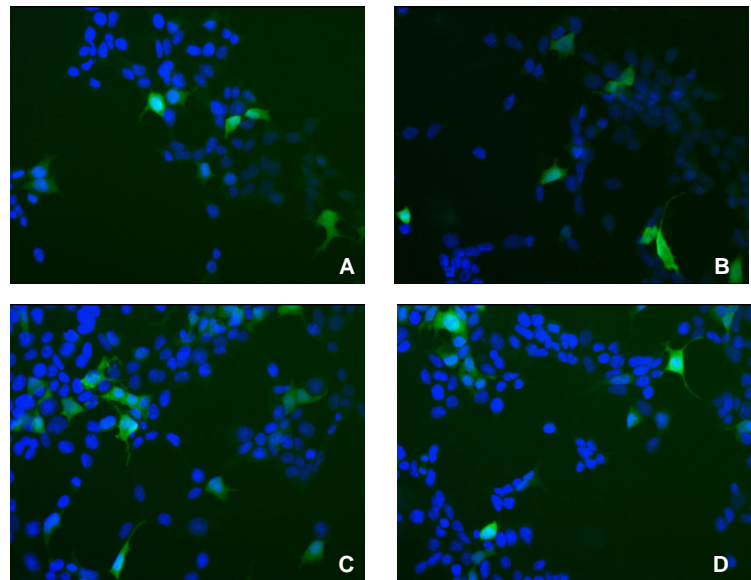
Figure1. Lentiviral titration in HEK293T cells by Immunofluorescence experiment. Panel A and B show representative images from the titration of ViraBind -concentrated (A) and un-concentrated (B) lentivirus, respectively. Panel C and D show representative images from the titration of Millipore-concentrated and un-concentrated lentivirus, respectively. Green stain represents cells positive to infection (GFP+); DAPI was used for nuclear staining.

In order to confirm the effective production of the mSlc7a1 lentivirus, we infected HEK293T cells with this virus at different MOI values (1, 2 and 2.5). Blasticid selection was started two days from infection using 2 different amounts (4 and 6 µg/ml) in order to determine the best concentration. After one week of selection, about 20-30% of cells infected at a MOI of 2.5 survived with both Blasticidin concentrations; these cells were expanded for some days and the DNA was extracted in order to perform a PCR with specific primers for the amplification of mSlc7a1. The PCR profile was positive further confirming the presence of mSlc7a1 lentiviral cassette in these cells (Fig.2).
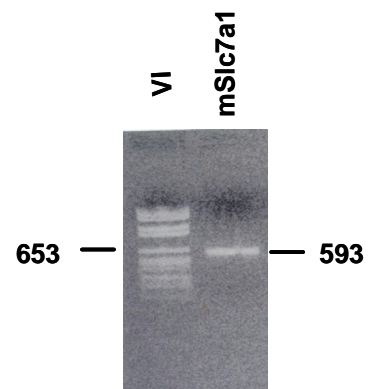
Figure 2. PCR amplification of mSlc7a1 lentiviral cassette. PCR was performed with primers specific for mSlc7a1 coding sequence. After amplification we obtained a band of 593bp as expected. Marker VI (Roche) was used to asses DNA molecular weight.

57

As a consequence of the low amount of virus obtained after concentration with both kits, we could not use concentrated virus for fibroblasts infection; in fact, to have a MOI of 2 (the minimal value suggested in the reprogramming protocol), we had to use a volume of viral preparation higher than that obtained after the concentration. Thus, we decided to proceed with the infection of primary fibroblasts using the un-concentrated lentiviral vectors despite the low viral titer.

Since we had to use un-concentrated virus, in order to maximise the efficacy of the infection and to obtain an higher percentage of cells infected by both EOS and mSlc7a1, we decided to modify the original protocol. Indeed, the protocol suggested to infect fibroblasts firstly with EOS lentiviral vector and after to proceed with mSlc7a1 infection and Blasticidin selection. We decided to start directly with mSlc7a1 infection (MOI of 2) and then to proceed with EOS lentiviral infection on cells surviving to Blasticidin selection, in order to maximize the number of EOS-infected cells (Fig.3).
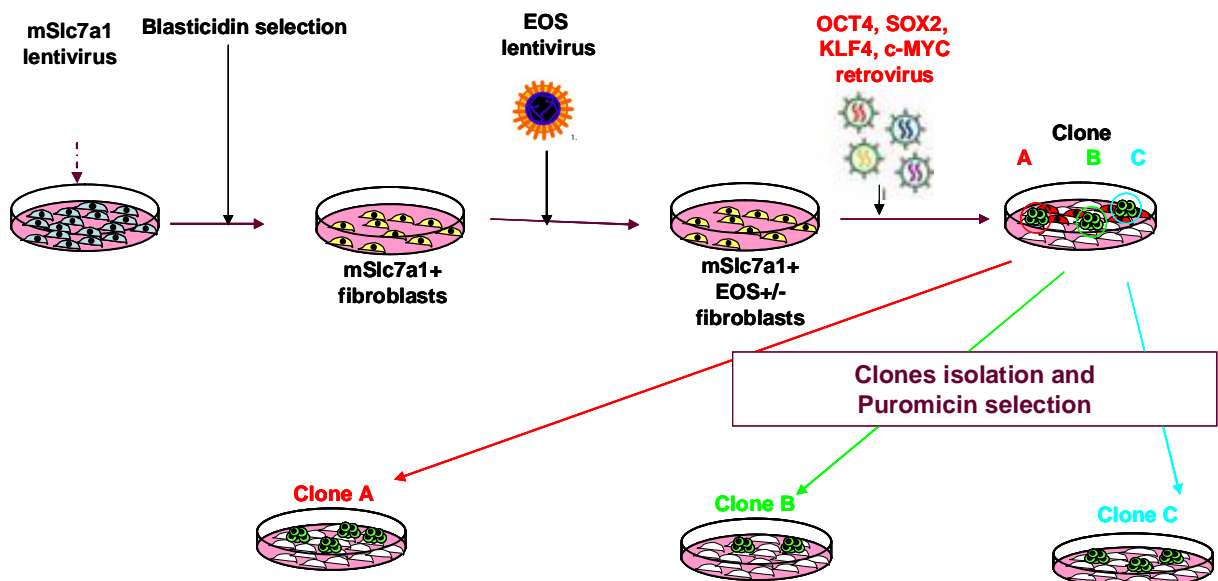
Figure 3. Schematic representation of the modified protocol. In order to maximize the efficacy of infection, cells were infected with the un-concentrated mSLC7a1 virus and then selected for resistance to Blasticidin. Selected cells were then infected with EOS lentivirus and finally the infection with the retrovirus carrying the Yamanaka's factors was performed to induce cellular reprogramming into iPSCs.

Fibroblasts infected with lentiviral vectors were then infected with reprogramming retroviral vectors two times. Seven days from infection, cells were seeded on Matrigel-coated dishes and fibroblast medium was substituted with mTeSR1 medium. Cells were maintained in mTeSR1 for more than a month but no morphological changes appeared and all cells died when Puromicin was added to culture medium. The procedure was repeated using the maximum possible MOI (2.5) but again no reprogrammed clones were obtained.

58

Taking into account the problems with the original protocol, we decided to generate iPS through the employment of the commercial STEMCCA Constitutive Polycistronic (OKSM) Lentivirus Kit (Millpore), supposing that the efficiency of the virus produced in our laboratory wasn't sufficient for reprogramming fibroblasts into iPS. This commercial lentiviral kit consists of a single lentiviral vector that allows the expression of the "stem cell cassette" comprised of all four transcription factors. The iPS induction through the use of a single lentiviral vector instead the four separate retrovirus vectors is reported to have a higher efficiency of reprogramming in addition to reduced risks of insertional mutagenesis and viral reactivation [77].

Following the STEMMCA protocol, 1×10^4 fibroblasts were infected with the virus at a MOI of 75 adding the viral preparation to medium containing 5 µg/ml Polybrene. To exclude that the failure of our previous reprogramming attempts could be caused by the haploinsuffiency of *FOXG1* gene in cells, we decided to include in the experiment fibroblasts from a patient carrying a *MECP2* mutation (p.T158M). Two infections in consecutive days were performed, as suggested by the protocol. Six days from infection cells were seeded on Matrigel-coated dishes and fibroblast medium was substituted with mTeSR1 medium. The experiment is still ongoing and some cellular morphological changes seem to appear.

6. RESULT-4

6.1 Introduction

FoxG1 is a transcription factor highly conserved in vertebrates where it has been evidenced in dividing progenitors of the ventricular zone and in early postmitotic neurons of the telecephalic neuroepitelium [78]. It is expressed from the earliest stages of telencephalic development through the adult and it is critical for the specification, differentiation and also the early cellular divisions in the telencephalon [78]. Genetic studies, using model organism such as mouse, have allowed identifying the transcription factors mainly involved in the patterning of the embryonic telencephalon. The expression of these transcriptional factors is essential for the definition of broad areas from which different cell types are generated that develop into functionally distinct structures [52]. Specifically, FoxG1 expression in mice occurs in part of the anterior neural plate at approximately E8.5 and it is involved in the dorso-ventral determination of the telencephalon acting both directly and indirectly in cooperation with other key transcription factors such as SHH and FGF [52,78]. In particular, the embryonic ventral telencephalon is induced by Foxg1 promotion of FGF expression, essential for the determination of ventral cell character[52]. Accordingly, Foxg1 Knock-Out (KO) mice show a premature differentiation in the dorsal telencephalon resulting in a loss of ventral cell types and a hypoplasia of the telencephalon [55].

Recently, *FOXG1* has been identified as the gene responsible for the congenital variant of Rett syndrome (RTT), a progressive neurodevelopmental disorder affecting mainly females (incidence 1: 10000) [31]. Since FoxG1 is a transcription factor, it is possible to hypothesize that the RTT phenotype of the mutated patients might result, at least in part, from mis-regulated gene expression. Up to now, functional studies based on a candidate gene approach have allowed to identify some target genes such as p27Xic in Xenopus and p21Cip, Bmp4 and Fgf8 in mouse[50,55,58,73]. In order to better define FoxG1 signaling cascade and to identify other candidate genes, we decided to perform a global expression profiling study in mutant heterozygous mice brain. Specifically, expression profiles of $Foxg1^{+/-}$ adult brain (P30) were compared to those of wild type age-matched brain samples to test whether FoxG1 deficiency results in a widespread alteration of gene expression.

6.2 Experimental procedures

Mice. The *FoxG1*^{+/-} mice were obtained from Dr. Vania Broccoli (San Raffaele Scientific Institue) who maintains in his laboratory a colony of the *Foxg-cre* animals originally developed by Hebert and McConnell (2000). These mice carry the Cre gene in the Foxg1 locus determining a complete replacement of the intron-less *Foxg1* coding region. The *Foxg1* mutant colony has been maintained by crossing *Foxg1* heterozygous mutants with B16/C57 wild-type animals. For the microarray experiments we analyzed 3 *FoxG1*^{+/-} mutants and 3 wild-type littermates at P30 age.

RNA isolation and quality control. Total brain tissue from wild-type and *FoxG1*^{+/-} mice were frozen in dry ice and total RNA was extracted using the Qiagen RNeasy Lipid Tissue mini kit (Qiagen) following manufacturer protocol. RNA quality, amount and degradation were verified using Agilent 2100 Bioanalyzer (Agilent Technologies). RNA integrity was evaluated by RIN (RNA Integrity Values) software algorithm; 10 different categories raging from 1 (worst) to 10 (best) are assigned to samples. We obtained values around 7.2 for all samples indicating a good RNA quality.

cDNA labeling and microarray hybridization. Total RNA (200 ng) from wild type and Foxg1 mutant samples were reverse transcribed and labeled with Cy3-dCTP and Cy5-dCTP respectively, using the Low Input QuickAmp Labeling Kit (Qiagen). Labeled cRNA was firstly purified using the Qiagen RNaeasy mini kit (Qiagen) following manufacturer protocol and then quantified using NanoDrop ND-1000 UV-VIS Spectrophotometer. Equal amounts (825 ng) of the labeled cRNAs were combined together into a hybridization reaction and were applied on Agilent Whole Mouse Genome 4 × 44K microarray platform (Agilent Technologies). Hybridization was carried out at 65°C for 17 hours in a hybridization oven.

Microarray data analysis. Following hybridization, microarrays were washed and immediately scanned with an Agilent DNA microarray scanner (G2505B) and analyzed by Agilent Feature Extraction Software v9.5. The resulting text files were imported into GeneSpring GX 11.5 (Agilent technologies) for the analysis. Differentially expressed genes were identified by a fold change analysis. This value gives the absolute ratio of normalized intensities (no log scale) between the average intensities of the samples grouped. We selected an entities list that satisfied a fold change cut off of 1.5.

6.3 Results

The present study represents a preliminary analysis of gene expression profiles in control and mutated Foxg1 Knock-Out (KO) mice with the aim to identify differentially expressed genes, associated with disease state, whose expression may be regulated directly or indirectly by FoxG1. For this experiment, hybridization of labeled RNA on Agilent Whole Mouse Genome 4 × 44K chips (Agilent Technologies) was carried out with three couples of WT/heterozygous brain samples (3 biological replicates) and for each couple 3 technical replicates were performed. After generating microarray scan images, the Feature Extraction 9.5 (FE) program automatically assign a microarray grid, flags outlier pixels and performs statistics on inlier pixels of features and background. The software flags the outlier and background and subtracts the background from features. Data files were then imported to GenSpring for further analyses (Fig. 1).
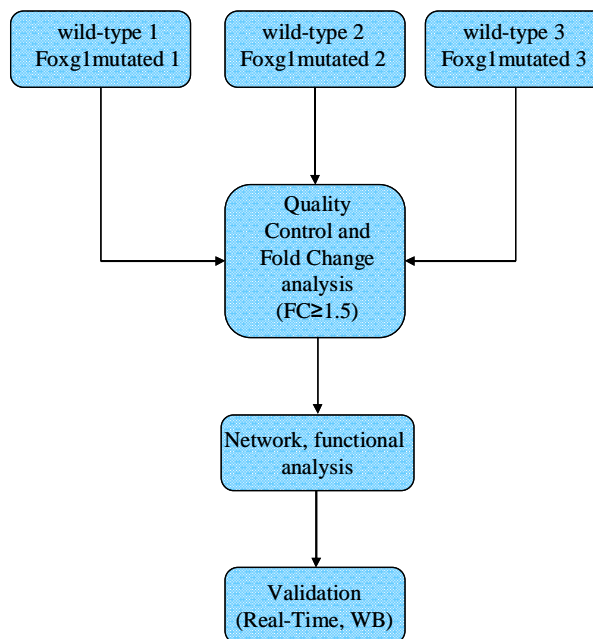
Figure 1. Flow chart summarizing the analysis procedures. Gene expression profiling was performed on 3 couples of wild type and Foxg1$^{+/-}$ mice using Agilent gene expression arrays. Data files were imported into GeneSpring GX 11.5 (Agilent technologies) and a quality control was performed to select all significant features. Fold Change analysis (cut off FC ≥ 1.5) was performed on the entities to select differentially expressed genes. Further, network and functional analysis was performed. Differentially regulated genes will be validated by Real Time PCR and Western Blot.

Once data files were imported into GeneSpring GX 11.5 (Agilent technologies), the technical replicates for each couple of brain samples were clustered together. In this way, we calculated differences in gene expression level between wt and mutant for each couple of samples separately (matched pairs). After grouping all data, we carried out a quality control, flagging as "compromised" and thus removing all probes that were not uniform and not above the background or had a saturated signal. For each probe, normalization was performed with the "baseline to median of all samples" option, in order to keep out all not reliable entities.

Starting from the resulting gene list, in order to select differentially expressed genes, we performed a Fold Change analysis setting a cut off value at 1.5. We obtained a list of 258 entities for the Entity list 1 (wt1 versus mutated1), a list of 198 entities for the Entity list 2 (wt2 versus mutated 2) and a list of 220 entities for the Entity list 3 (wt3 versus mutated 3). To visualize the common entities between the three gene lists we used the Venn Diagram Operation, but no entities common to all 3 samples resulted (Fig.2).
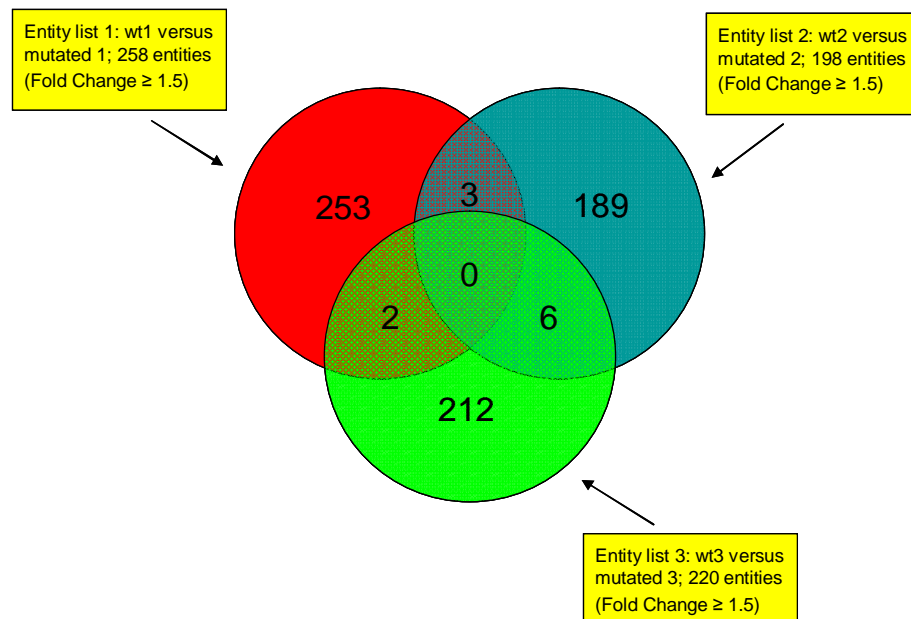
Figure 2. Venn Diagram among the three entity lists. After Fold Change analysis an entity list of differentially expressed genes was obtained for each couple of samples (WT vs mutant brain) used in the microarray. Comparing these lists by Venn Diagram Option a list composed by 11 genes (entities) common to 2 out of 3 samples was extrapolated.

We thus decided to consider all entities shared in at least two of three lists and we identified 11 genes. On these genes we performed a functional gene analysis in order to select relevant genes that might be associated with disease state and with Foxg1 signaling on the basis of their function (Table 1). As indicated in table 1, 10 out of 11 genes are down-

regulated. Three genes belong to the large superfamily of the olfactory receptors and they have been excluded from further analysis given their high variability in the population [79]. Among the remaining genes, Vit, Ms4a10 and Ttc18 genes seems to be particularly interesting on the basis of their molecular function. In fact, they are involved in cell adhesiveness, signal transduction and transcriptional control and neurogenesis, respectively.

Gene Symbol	Gene Name	Fold Change	Gene Bank no.	Description
Vit	Vitrin	-2.5516617	NM_028813	Promotes matrix assembly and cell adhesiveness, binds dermatan sulphate and chondriotin sulphate.
Ttc18	tetratricopeptide repeat domain 18	-1.8720530	NM_001163638	TTC18 is a protein of unknown function that belongs to the tetratrico peptide repeat (TPR) family. Contains seven TPR domains. TPRs are involved in a variety of biological processes, such as cell cycle regulation, transcriptional control, neurogenesis, protein folding mitochondrial and peroxisomal protein transport.
Ms4a10	membrane-spanning 4-domains, subfamily A, member 10	-1.8039613	NM_023529	May be involved in signal transduction as a component of a multimeric receptor complex. It is expressed in thymus, kidney, colon, brain and testis and also by various hematopoietic and lymphoblastoid cell lines.
Znrf4	zinc and ring finger 4	-1.7663639	NM_011483	Not better defined
Cgnl1	cingulin-like 1	-1.7462954	NM_026599	The mouse homolog of CGNL1 has been designated JACOP (junction-associated coiled-coil protein). JACOP is recruited to the junctional complex in epithelial cells and to cell-cell contacts in fibroblasts. It has been suggested that JACOP is involved in anchoring cell-cell contacts to actin-based cytoskeletons within cells
Trmt2a (Htf9c)	TRM2 tRNA methyltransferase 2 homolog A	-1.6402607	NM_001080999	Widely expressed at low level. Expressed at higher level in proliferating cells. Transcription is activated at the G1/S transition of the cell cycle and peaks in S phase, while being repressed in quiescent tissues and growth-arrested cells. Htf9a (RanBP1) and Trmt2a are transcribed with opposite polarity from complementary DNA strands from a shared bidirectional TATA-less promoter.
Stk32a	serine/threonine kinase 32A	-1.5620961	NM_178749	Belongs to the protein Ser/Thr protein kinase superfamily.
Olfr651	olfactory receptor 651	-2.3789212	NM_146813	The olfactory receptor proteins are members of a large family of G-protein-coupled receptors (GPCR) arising from single coding-exon genes. Olfactory receptors share a 7-transmembrane domain structure with many neurotransmitter and hormone receptors and are responsible for the recognition and G protein-mediated transduction of odorant signals. The olfactory receptor gene family is the largest in the genome. The nomenclature assigned to the olfactory receptor genes and proteins for this organism is independent of other organisms.
Olfr247	olfactory receptor 247	-1.7875498	NM_146269	Refer to Olfr651
Olfr17	olfactory receptor 17	-1.7521043	NM_020598	Refer to Olfr651
Neu1	neuraminidase 1	1.5519451	NM_010893	Lysosomal-type sialidases

Table 1. Genes with a Fold Change (FC) of 1.5 or greater (in either direction) are displayed in this table. FC negative values indicate that the expression is down-regulated in mutant brain. FC positive values indicate that the expression is up-regulated.

7. CONCLUSIONS & FUTURE PERSPECTIVE

In 2008 our group described in a clinical report a case of a 7-year-old patient that presented severe mental retardation, epilepsy, microcephaly and Rett-like features [37]. Array-CGH analysis allowed to identify in the patient a pathogenic de novo deletion in 14q12 containing a low number of genes. Functional analysis of these genes evidenced *FOXG1* as strong candidate disease gene considering that it encodes for a transcriptional factor with a brain restricted expression. Subsequently, additional *FOXG1* mutations was reported by Ariani et al in two *MECP2* mutation- negative patients with a clinical phenotype resembling the congenital variant of Rett Syndrome (RTT), suggesting that the gene could be responsible for this severe RTT variant [31]. In order to confirm *FOXG1* role in congenital RTT development and to better define the phenotypic spectrum associated with mutations in this gene, we expanded the mutational analysis to other patients obtained from an international collaboration and four additional patients with *FOXG1* mutations were identified (Result 1). Additional mutations have been subsequently identified by other groups. At present, the literature reports 12 intragenic mutations in *FOXG1* gene [31,41,42,80] (Table 1). Very recently, Kortum and colleagues reported 5 additional point mutations and presented an extensive clinical evaluation of *FOXG1* mutated patients [44] (Table 1). They suggested that heterozygous loss of *FOXG1* lead to a severe developmental disorder with widely variable clinical features that overlap with other developmental encephalopathies beyond RTT. However, they also identified a specific combination of developmental and brain imaging features that define a clinically recognizable phenotype that authors designated as "*FOXG1* syndrome" [44].

Further confirming the phenotypic variability associated to *FOXG1* mutations, we report here two unrelated patients with de novo *FOXG1* point mutations (p.Q6X and Y400X) exhibiting a phenotype that does not fit with either classic or variant RTT. In fact, these patients present many characteristics resembling RTT phenotype, such as normal prenatal and perinatal period, postnatal microcephaly and hand stereotypies, but they had quite good motor abilities and were able to walk. This finding further expands the phenotypic spectrum associated to *FOXG1* mutation. The combination of these data with other literature reports regarding the phenotype heterogeneity of *FOXG1* mutated patients suggests that a better definition of the genotype-phenotype correlation is still necessary.

FoxG1 is a transcriptional regulator involved in global chromatin organization and it plays a key role in regulating neuronal differentiation. However, the relationship between FoxG1 and chromatin and its functional role in the nucleus have not been elucidated. In order to clarify the pathogenic mechanisms of *FOXG1*-associated disorders, we thus decided to examine the relationship between FoxG1 and chromatin (Result 2). Applying strip-FRAP experiments, we tested and compared the distribution, binding and mobility of three FoxG1 derivatives, two mutations correlated to a milder phenotype (p.Q46X and p.Y400X) and a previously reported mutation associated with the congenital variant (p.Ser323fsX325), in order to verify whether a milder phenotype could be associated with specific mutations. The functional characterization of the protein revealed that FoxG1 binding to chromatin is reversible even if a significant fraction of the total protein is stably bound. These findings allowed us to speculate on the possible different roles of FoxG1 in the nucleus and their relationship to disease mechanisms. While the reversibly-bound fraction might be associated with dynamic regulation of gene expression, the stably bound fraction might be involved in the structural organization of the chromatin. Our data indicated that protein integrity is crucial to determine chromatin binding since the reduction in chromatin affinity further decreased with the extension of deletion. Intriguingly, our results suggest that the severity of RTT symptoms might be determined by the fraction of FoxG1 protein stably bound to chromatin (the immobile fraction - IF). In fact, IF value appear significantly higher for the mutation p.Ser323fsX325, that is associated to most severe RTT phenotype.

Considering that RTT patients are heterozygotes for *FOXG1* mutation, it is important to remind that mutated protein compete with wt protein for interaction with chromatin. On the basis of our results, it is thus tempting to speculate that the severity of the symptoms could be attributed to the amount of mutated protein fraction that is stably bound to chromatin and thus prevents the access to chromatin of the wt protein. Specifically, the IF of some pathological derivatives, such us p.Ser323fsX325, could partially or completely exclude wt FoxG1 protein from chromatin thus preventing its correct function. On the contrary, the more N-terminal mutations (such as the p.Q46X) have a reduced capacity to stably bind chromatin and thus they are not expected to impair the activity of wt FoxG1 protein. As a consequence, wild type FoxG1, although in lower amount, might still be able to interact with chromatin resulting in a partial maintenance of its regulatory functions resulting in a milder phenotype. Further experiments with additional pathological derivatives will be essential to confirm these hypotheses and to better clarify the protein domains functionally involved in chromatin binding.

Up to now, the investigation of molecular mechanisms of neurodevelopmental and neurodegenerative disorders, such as RTT, was performed mainly using mouse models. For *FOXG1* gene these models have been extensively studied and they have given important insights into the function of the protein in brain development. However, despite these models represent a useful tool, they do not faithfully recapitulate human conditions and do not take into account the influence of genetic background on disease phenotype. It will be thus essential to develop good human cellular models, to confirm the relevance of alterations identified in animal models for human disease mechanisms. To this aim, an innovative approach based on genetic reprogramming has been recently developed to generate embryonic stem (ES) like cells, named induced pluripotent stem cells (iPSCs), from primary human fibroblasts. This revolutionary technology gives the opportunity to recapitulate pathologic human tissues formation in vitro and it is thus the ideal tool to study neurological disorders directly on neurons, that represent the primarily affected cells. Therefore, we decided to utilize this technology to obtain iPSCs from *FOXG1*-mutated fibroblasts. Unfortunately, our first attempts did not succeed, probably due to a technical problem related to the concentration of the lentivirus. We thus decided to use a commercial system, the STEMMCA Constitutive Polycistronic (OKMS) Lentiviral Kit (Millipore), to overcome this limitation. The reprogramming experiment is still ongoing. Once reprogrammed cells will be available, it will be interesting to check whether we can recapitulate in patient-specific neurons the alterations in FoxG1-chromatin interaction observed with FoxG1-derivatives (Results 3).

FOXG1 encodes for a transcription factor specifically expressed in fetal and adult brain. Important advances in understanding FoxG1 function during neuronal differentiation have been performed mainly by studies on mouse models. However, at the moment very little is know about the target genes of FoxG1. In order to better define FoxG1 signaling cascade, we thus decided to perform a global transcriptional profiling comparing P30 wild-type and $Foxg1^{+/-}$ mouse brain. The final goal was to identify genes associated with the disease state whose expression is directly or indirectly regulated by Foxg1. Our analysis returned a list of 11 differentially expressed genes (Result 4).

Among these genes, we observed a significant down-regulation of Ttc18 gene. This gene is particularly interesting since it seems to be involved in several biological processes including cell cycle regulation, transcriptional control and neurogenesis. Considering that FoxG1 is a transcriptional regulator involved in regulating the proliferation of neural progenitor cells, it is tempting to speculate that it might exert its effect in part through the regulation of Ttc18 expression; the haploinsufficiency of Ttc18 could thus be one of the

possible factors responsible for the severe volume reduction of the cerebral cortex, striatum and hippocampus characteristic of $Foxg1^{+/-}$ mice tissues. Moreover, we observed a significant decrease in the expression of Ms4a10 gene encoding for a factor involved in signal transduction as a component of a multimeric receptor complex. The protein is expressed in thymus, kidney, colon, brain and testis. Apart from its tissue distribution, no many informations are known about this protein. However, considering that FoxG1 is a transcriptional regulator whose expression is restricted to brain and testis, the partial loss of gene activity in $Foxg1^{+/-}$ mice could be consistent with a down-regulation of Ms4a10 gene. Finally, we found a significant downregulation of Vitrin, a protein involved in extracellular matrix assembly and cell adhesiveness that might participate in orchestrating extracellular environmental signals for cell fate determination and tissue patterning.

These preliminary results allowed us to identify only a limited number of differentially expressed genes respect to those usually obtained from expression profiling experiments reported in literature. A possible explanation might reside in the fact that the expression profiling experiment has been performed using heterozygous mice. We thus expected that effects on gene expression profiles would be milder considering that the *FOXG1* wt allele partially compensate for the functional absence of the mutated allele and thus only the strongest effects are visible. More consistent results could be probably obtained from studies on *FOXG1* homozygous mice. However, the principal limitation to these experiments is represented by the difficulty to generate homozygous mice since that mice die perinatally and they have a strongly reduced and compromised telencephalon. An other possible explanation to the limited number of dis-regulated genes identified could be the fact that we used total mouse brain tissue. In fact, it is possible that FoxG1 deficiency might exert its deleterious effects on specific cell types or brain regions, as seems to be the case for MeCP2 deficiency [19]. If this is the case, the use of total brain tissue might dilute the effect of *FOXG1* deficiency in individual brain regions, thus masking relevant expression differences. In this respect it will be thus important to analyze specific brain regions. Moreover, further insights into the transcriptional network regulated by FoxG1 might come from the analysis of patient-specific neurons, once iPSCs from our *FOXG1*-mutated patients will be available. In the meantime, the extension of the analysis to a larger number of samples will likely allow to confirm the relevance of the identified genes and possibly to identify additional differentially expressed genes.

In conclusion, this work allowed us to confirm the pathogenic role of *FOXG1* gene in the congenital variant of RTT and to further expand the characterization of its phenotypic

spectrum (Results 1 & 2). Moreover, cellular biology experiments have highlighted specific effects of FoxG1 mutation on the interaction with chromatin (Result 2). Preliminary gene expression profiling experiments let us to identify possible target genes of FoxG1 regulation. (Result 4). At present, genetic reprogramming experiments on fibroblasts obtained from *FOXG1*-mutated patients are in place in order to produce iPSCs and then induce neuronal differentiation (Result 3). These cells will allow to confirm the obtained results on a human model.

PHENOTYPE	AGE	SEX	*FOXG1* MUTATION	MUTATION TYPE	REFERENCE
Congenital variant of RTT	22y	F	c.765G>A; p.W255X	nonsense	Ariani et al., 2008[31]
Congenital variant of RTT	7y	F	c.969delC; p.S323fsX325	frameshift	Ariani et al., 2008[31]
Congenital variant of RTT	13y2m	F	c.681C>G; p.N227K	missense	Mencarelli et al., 2010 (Result 1)
Congenital variant of RTT	8y	F	c.643T>C; p.F215L	missense	Mencarelli et al., 2010 (Result 1)
Congenital variant of RTT	3y	F	c.551_552insC; p.S185fsX454	frameshift	Mencarelli et al., 2010 (Result 1)
Congenital variant of RTT	3y2m	F	c.624C>G; p.Y208X	nonsense	Mencarelli et al., 2010 (Result 1)
Congenital variant of RTT	22y	F	c.924A>G; p.W308X	nonsense	Philippe et al., 2010[41]
Classic RTT	10y	F	c.1200C>G; p.Y400X	nonsense	Philippe et al., 2010[41]
Congenital variant of RTT	4y	F	c.1248C>G; p.Y416X	nonsense	Bahi-Buisson et al., 2010[40]
Congenital variant of RTT	5y8m	F	c.460_461dupG; p.E154GfsX300	frameshift	Bahi-Buisson et al., 2010[40]
Congenital variant of RTT	8y	F	c.730C>T; p.R244C	missense	Le Guen et al., 2010[43]
Congenital variant of RTT	3y	M	c.256-257dupC p.Q86PfsX34	frameshift	Le Guen et al., 2011[42]
FOXG1 syndrome	16y	F	c.757A>G; p.N253D	missense	Kortüm et al.,2011[44]
FOXG1 syndrome	18y	M	c.700T>C; p.S234P	missense	Kortüm et al.,2011[44]
FOXG1 syndrome	31y	F	c.256C>T; p.R86X	nonsense	Kortüm et al.,2011[44]
FOXG1 syndrome	10y8m	M	c.505_506delGGinsT; p.G168fsX23	frameshift	Kortüm et al.,2011[44]
FOXG1 syndrome	5y	M	c.263_278del16; p.R88PfsX99	frameshift	Kortüm et al.,2011[44]

Table 1. *FOXG1* point mutations present in the literature

8. REFERENCES

1   Rett A: Ueber ein eigenartiges hirnatrophisches Syndrom bei Hyperammonaemie im Kindesalter. *Wien.Med.Wochenschrift* 1966; **116**: 723-726.

2   Hagberg B, Aicardi J, Dias K, Ramos O: A progressive syndrome of autism, dementia, ataxia, and loss of purposeful hand use in girls: Rett's syndrome: report of 35 cases. *Ann Neurol* 1983; **14**: 471-479.

3   Matsuishi T, Yamashita Y, Takahashi T, Nagamitsu S: Rett syndrome: the state of clinical and basic research, and future perspectives. *Brain Dev* 2011; **33**: 627-631.

4   Chahrour M, Zoghbi HY: The story of Rett syndrome: from clinic to neurobiology. *Neuron* 2007; **56**: 422-437.

5   Meloni I, Bruttini M, Longo I *et al*: A mutation in the Rett syndrome gene, *MECP2*, causes X-linked mental retardation and progressive spasticity in males. *Am J Hum Genet* 2000; **67**: 982-985.

6   Artuso R: Early-onset seizure variant of Rett syndrome: Definition of the clinical diagnostic criteria. *Brain and Development* 2010; **32**: 17-24.

7   Beyer KS, Blasi F, Bacchelli E, Klauck SM, Maestrini E, Poustka A: Mutation analysis of the coding sequence of the MECP2 gene in infantile autism. *Hum Genet* 2002; **111**: 305-309.

8   Hagberg BA. Rett Syndrome - Clinical & Biological aspects. London, McKeith Press, 1993.

9   Christodoulou J, Ho G. MECP2-Related Disorders; in: Pagon RA BT, Dolan CR, Stephens K (ed): GeneReviews. Seattle (WA), University of Washington, 2001.

10   Sampieri K, Meloni I, Scala E *et al*: Italian Rett database and biobank. *Hum Mutat* 2007; **28**: 329-335.

11   Archer HL, Whatley SD, Evans JC *et al*: Gross rearrangements of the MECP2 gene are found in both classical and atypical Rett syndrome patients. *J Med Genet* 2006; **43**: 451-456.

12   Pan H, Li MR, Nelson P, Bao XH, Wu XR, Yu S: Large deletions of the MECP2 gene in Chinese patients with classical Rett syndrome. *Clin Genet* 2006; **70**: 418-419.

13   Hendrich B, Bird A: Identification and characterization of a family of mammalian methyl-CpG binding proteins. *Mol.Cell.Biol.* 1998; **18**: 6538-6547.

14   Nan X, Ng H, Johnson C *et al*: Transcriptional repression by the methyl-CpG-binding protein MeCP2 involves a histone deacetylase complex. *Nature* 1998; **393**: 386-389.

15   Kokura K, Kaul S, Wadhwa R *et al*: The Ski protein family is required for MeCP2-mediated transcriptional repression. *J Biol Chem.* 2001; **276**: 34115-34121.

16   Kaludov NK, Wolffe AP: MeCP2 driven transcriptional repression in vito: selectivity for methylated DNA, action at a distance and contacts with the basal transcription machinery. *Nucleic Acids Research* 2000; **28**: 1921-1928.

17   Horike S, Cai S, Miyano M, Cheng J, Kohwi-Shigematsu T: Loss of silent-chromatin looping and impaired imprinting of DLX5 in Rett syndrome. *Nat Genet* 2005; **37**: 31-40.

18   Young JI, Hong EP, Castle JC *et al*: Regulation of RNA splicing by the methylation-dependent transcriptional repressor methyl-CpG binding protein 2. *Proc Natl Acad Sci U S A* 2005; **102**: 17551-17558.

19   Chahrour M, Jung SY, Shaw C *et al*: MeCP2, a key contributor to neurological disease, activates and represses transcription. *Science* 2008; **320**: 1224-1229.

20   Scala E, Ariani F, Mari F *et al*: CDKL5/STK9 is mutated in Rett syndrome variant with infantile spasms. *J Med Genet* 2005; **42 (2)**: 103-107.

21   Tao J, Van Esch H, Hagedorn-Greiwe M *et al*: Mutations in the X-linked cyclin-dependent kinase-like 5 (CDKL5/STK9) gene are associated with severe neurodevelopmental retardation. *Am J Hum Genet.* 2004; **75**: 1149-1154.

22   Mari F, Azimonti S, Bertani I *et al*: CDKL5 belongs to the same molecular pathway of MeCP2 and it is responsible for the early-onset seizure variant of Rett syndrome. *Hum Mol Genet.* 2005; **14**: 1935-1946.

23   Evans J, Archer H, Colley J *et al*: Early onset seizures and Rett-like features associated with mutations in CDKL5. *Eur J Hum Genet* 2005; **13**: 1113-1120.

24   Nectoux J, Heron D, Tallot M, Chelly J, Bienvenu T: Maternal origin of a novel C-terminal truncation mutation in CDKL5 causing a severe atypical form of Rett syndrome. *Clin Genet* 2006; **70**: 29-33.

25   Sprovieri T, Conforti FL, Fiumara A *et al*: A novel mutation in the X-linked cyclin-dependent kinase-like 5 (CDKL5) gene associated with a severe Rett phenotype. *Am J Med Genet A* 2009; **149A**: 722-725.

26   Montini E, Andolfi G, Caruso A *et al*: Identification and characterization of a novel serine-threonine kinase gene from the Xp22 region. *Genomics* 1998; **51**: 427-433.

27   Rusconi L, Salvatoni L, Giudici L *et al*: CDKL5 expression is modulated during neuronal development and its subcellular distribution is tightly regulated by the C-terminal tail. *J Biol Chem* 2008; **283**: 30101-30111.

28   Lin C, Franco B, Rosner MR: CDKL5/Stk9 kinase inactivation is associated with neuronal developmental disorders. *Hum Mol Genet* 2005; **14**: 3775-3786.

29   Bertani I, Rusconi L, Bolognese F *et al*: Functional consequences of mutations in CDKL5, an X-linked gene involved in infantile spasms and mental retardation. *J Biol Chem* 2006; **281**: 32048-32056.

30   Carouge D, Host L, Aunis D, Zwiller J, Anglard P: CDKL5 is a brain MeCP2 target gene regulated by DNA methylation. *Neurobiol Dis* 2010; **38**: 414-424.

31   Ariani F, Hayek G, Rondinella D *et al*: FOXG1 is responsible for the congenital variant of Rett syndrome. *Am J Hum Genet* 2008; **83**: 89-93.

32   Neul J, Kaufmann W, Glaze D *et al*: Rett Syndrome: Revised Diagnostic Criteria and Nomenclature. *Annals of Neurology* 2010; **in press**.

33   Renieri A, Mari F, Mencarelli MA *et al*: Diagnostic criteria for the Zappella variant of Rett syndrome (the preserved speech variant). *Brain Dev* 2009; **31**: 208-216.

34   Zappella M, Meloni I, Longo I *et al*: *Study of MECP2 gene in Rett syndrome variants and autistic girls. Am J Med Genet (Neuropsychiatr Genet)* 2003; **119B**: 102-107.

35   Shoichet SA, Kunde SA, Viertel P *et al*: Haploinsufficiency of novel FOXG1B variants in a patient with severe mental retardation, brain malformations and microcephaly. *Hum Genet* 2005; **117**: 536-544.

36   Bisgaard AM, Kirchhoff M, Tumer Z *et al*: Additional chromosomal abnormalities in patients with a previously detected abnormal karyotype, mental retardation, and dysmorphic features. *Am J Med Genet A* 2006; **140**: 2180-2187.

37   Papa FT, Mencarelli MA, Caselli R *et al*: A 3 Mb deletion in 14q12 causes severe mental retardation, mild facial dysmorphisms and Rett-like features. *Am J Med Genet A* 2008; **146A**: 1994-1998.

38   Mencarelli MA, Kleefstra T, Katzaki E *et al*: 14q12 Microdeletion syndrome and congenital variant of Rett syndrome. *Eur J Med Genet* 2009; **52**: 148-152.

39   Rolando S: Rett syndrome: report of eight cases. *Brain and Development* 1985; **7**: 290-296.

40   Bahi-Buisson N, Nectoux J, Girard B *et al*: Revisiting the phenotype associated with FOXG1 mutations: two novel cases of congenital Rett variant. *Neurogenetics* 2010; **11**: 241-249.

41   Philippe C, Amsallem D, Francannet C *et al*: Phenotypic variability in Rett syndrome associated with FOXG1 mutations in females. *J Med Genet* 2009.

42   Le Guen T, Bahi-Buisson N, Nectoux J *et al*: A FOXG1 mutation in a boy with congenital variant of Rett syndrome. *Neurogenetics* 2010.

43   Le Guen T, Fichou Y, Nectoux J *et al*: A missense mutation within the fork-head domain of the forkhead box G1 Gene (FOXG1) affects its nuclear localization. *Hum Mutat* 2011; **32**: E2026-2035.

44   Kortum F, Das S, Flindt M *et al*: The core FOXG1 syndrome phenotype consists of postnatal microcephaly, severe mental retardation, absent language, dyskinesia, and corpus callosum hypogenesis. *J Med Genet* 2011; **48**: 396-406.

45   Yao J, Lai E, Stifani S: The winged-helix protein brain factor 1 interacts with groucho and hes proteins to repress transcription. *Mol Cell Biol* 2001; **21**: 1962-1972.

46   Dastidar SG, Landrieu PM, D'Mello SR: FoxG1 promotes the survival of postmitotic neurons. *J Neurosci* 2011; **31**: 402-413.

47   Hanashima C, Shen L, Li SC, Lai E: Brain factor-1 controls the proliferation and differentiation of neocortical progenitor cells through independent mechanisms. *J Neurosci* 2002; **22**: 6526-6536.

48   Seoane J, Le HV, Shen L, Anderson SA, Massague J: Integration of Smad and forkhead pathways in the control of neuroepithelial and glioblastoma cell proliferation. *Cell* 2004; **117**: 211-223.

49   Dou C, Lee J, Liu B *et al*: BF-1 interferes with transforming growth factor beta signaling by associating with Smad partners. *Mol Cell Biol* 2000; **20**: 6201-6211.

50   Seoane J: p21(WAF1/CIP1) at the switch between the anti-oncogenic and oncogenic faces of TGFbeta. *Cancer Biol Ther* 2004; **3**: 226-227.

51   Tao W, Lai E: Telencephalon-restricted expression of BF-1, a new member of the HNF-3/fork head gene family, in the developing rat brain. *Neuron* 1992; **8**: 957-966.

52   Hebert JM, Fishell G: The genetics of early telencephalon patterning: some assembly required. *Nat Rev Neurosci* 2008; **9**: 678-685.

53   Manuel M, Martynoga B, Yu T, West JD, Mason JO, Price DJ: The transcription factor Foxg1 regulates the competence of telencephalic cells to adopt subpallial fates in mice. *Development* 2010; **137**: 487-497.

54   Huh S, Hatini V, Marcus RC, Li SC, Lai E: Dorsal-ventral patterning defects in the eye of BF-1-deficient mice associated with a restricted loss of shh expression. *Dev Biol* 1999; **211**: 53-63.

55   Martynoga B, Morrison H, Price DJ, Mason JO: Foxg1 is required for specification of ventral telencephalon and region-specific regulation of dorsal telencephalic precursor proliferation and apoptosis. *Dev Biol* 2005; **283**: 113-127.

56   Hanashima C, Li SC, Shen L, Lai E, Fishell G: Foxg1 suppresses early cortical cell fate. *Science* 2004; **303**: 56-59.

57   Muzio L, Mallamaci A: Foxg1 confines Cajal-Retzius neuronogenesis and hippocampal morphogenesis to the dorsomedial pallium. *J Neurosci* 2005; **25**: 4435-4441.

58   Dou CL, Li S, Lai E: Dual role of brain factor-1 in regulating growth and patterning of the cerebral hemispheres. *Cereb Cortex* 1999; **9**: 543-550.

59   Xuan S, Baptista CA, Balas G, Tao W, Soares VC, Lai E: Winged helix transcription factor BF-1 is essential for the development of the cerebral hemispheres. *Neuron* 1995; **14**: 1141-1152.

60   Shen L, Nam HS, Song P, Moore H, Anderson SA: FoxG1 haploinsufficiency results in impaired neurogenesis in the postnatal hippocampus and contextual memory deficits. *Hippocampus* 2006; **16**: 875-890.

61   Marchetto MC, Winner B, Gage FH: Pluripotent stem cells in neurodegenerative and neurodevelopmental diseases. *Hum Mol Genet* 2010; **19**: R71-76.

62   Takahashi K, Tanabe K, Ohnuki M *et al*: Induction of pluripotent stem cells from adult human fibroblasts by defined factors. *Cell* 2007; **131**: 861-872.

63   Yamanaka S, Takahashi K: [Induction of pluripotent stem cells from mouse fibroblast cultures]. *Tanpakushitsu Kakusan Koso* 2006; **51**: 2346-2351.

64   Vaccarino FM, Stevens HE, Kocabas A *et al*: Induced pluripotent stem cells: a new tool to confront the challenge of neuropsychiatric disorders. *Neuropharmacology* 2011; **60**: 1355-1363.

65   Kim K, Doi A, Wen B *et al*: Epigenetic memory in induced pluripotent stem cells. *Nature* 2010; **467**: 285-290.

66   Boland MJ, Hazen JL, Nazor KL *et al*: Adult mice generated from induced pluripotent stem cells. *Nature* 2009; **461**: 91-94.

67   Chamberlain SJ, Li XJ, Lalande M: Induced pluripotent stem (iPS) cells as in vitro models of human neurogenetic disorders. *Neurogenetics* 2008; **9**: 227-235.

68   Urbach A, Bar-Nur O, Daley GQ, Benvenisty N: Differential modeling of fragile X syndrome by human embryonic stem cells and induced pluripotent stem cells. *Cell Stem Cell* 2010; **6**: 407-411.

69   Dimos JT, Rodolfa KT, Niakan KK *et al*: Induced pluripotent stem cells generated from patients with ALS can be differentiated into motor neurons. *Science* 2008; **321**: 1218-1221.

70   Ebert AD, Yu J, Rose FF, Jr. *et al*: Induced pluripotent stem cells from a spinal muscular atrophy patient. *Nature* 2008.

71   Marchetto MC, Carromeu C, Acab A *et al*: A model for neural development and treatment of Rett syndrome using human induced pluripotent stem cells. *Cell* 2010; **143**: 527-539.

72   Cheung AY, Horvath LM, Grafodatskaya D *et al*: Isolation of MECP2-null Rett Syndrome patient hiPS cells and isogenic controls through X-chromosome inactivation. *Hum Mol Genet* 2011; **20**: 2103-2115.

73   Hardcastle Z, Papalopulu N: Distinct effects of XBF-1 in regulating the cell cycle inhibitor p27(XIC1) and imparting a neural fate. *Development* 2000; **127**: 1303-1314.

74   Eagleson KL, Schlueter McFadyen-Ketchum LJ, Ahrens ET *et al*: Disruption of Foxg1 expression by knock-in of cre recombinase: effects on the development of the mouse telencephalon. *Neuroscience* 2007; **148**: 385-399.

75   Siegenthaler JA, Tremper-Wells BA, Miller MW: Foxg1 haploinsufficiency reduces the population of cortical intermediate progenitor cells: effect of increased p21 expression. *Cereb Cortex* 2008; **18**: 1865-1875.

76   Hotta A, Cheung AY, Farra N *et al*: EOS lentiviral vector selection system for human induced pluripotent stem cells. *Nat Protoc* 2009; **4**: 1828-1844.

77   Sommer CA, Stadtfeld M, Murphy GJ, Hochedlinger K, Kotton DN, Mostoslavsky G: Induced pluripotent stem cell generation using a single lentiviral stem cell cassette. *Stem Cells* 2009; **27**: 543-549.

78   Roth M, Bonev B, Lindsay J *et al*: FoxG1 and TLE2 act cooperatively to regulate ventral telencephalon formation. *Development* 2010; **137**: 1553-1562.

79   Keller A, Zhuang H, Chi Q, Vosshall LB, Matsunami H: Genetic variation in a human odorant receptor alters odour perception. *Nature* 2007; **449**: 468-472.

80   Bahi-Buisson N, Nectoux J, Girard B *et al*: Revisiting the phenotype associated with FOXG1 mutations: two novel cases of congenital Rett variant. *Neurogenetics* 2009; **11**: 241-249.

ACNOWLEDGMENTS

I will be brief and concise.

First, I would like to give a special thanks to all Rett Patients and their Family for the faith on scientific efforts; they represent the main incentive to work with passion and dedication.

Then, I thanks all my family for their support during these long years spent in Siena. They teach me that working hardly and seriously always gives the expected results.

Unexpectedly, an important person entered into my life and he has been a consistent daily presence, fundamental to my psychological and emotional stability in these last efforts. He has shown me that if you believe on something nothing is impossible neither to change the perception of space and time.

Finally, I would like to thanks prof. Alessandra Renieri, who gives me the possibility to work at an important and ambitious project, doc. Ilaria Meloni, who follows me with patience sharing her professional experiences and all the Genetic Team for their happiness and cakes!